Global Ocean Repeat Hydrography Study: pH and Total Alkalinity Measurements in the Atlantic Ocean A16 North and South Aug 2013 – Feb 2014

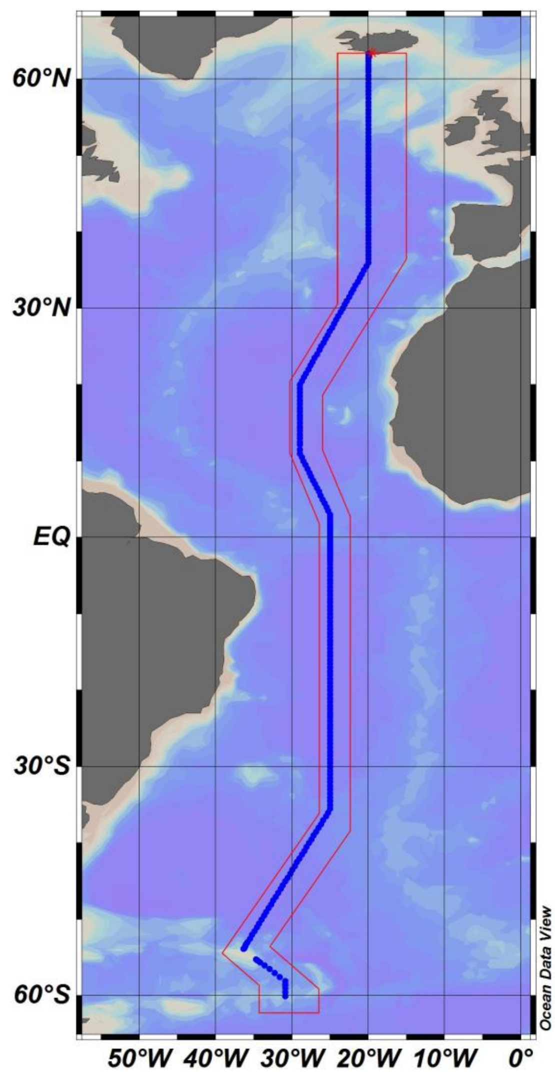

Frank J. Millero, Jonathan Sharp, Ryan J. Woosley, Carmen Rodriguez, Julia Paine, Josh Levy, James Williamson, Jennifer Byrne, and Kristen Mastropole

University of Miami, Rosenstiel School of Marine and Atmospheric Science
4600 Rickenbacker Causeway
Miami, FL 33149

Table of Contents

List of Tables

List of Figures

1. Introduction

The A16N and A16S cruises are comprised of a nearly complete north-south transect down the Atlantic Ocean beginning off the coast of Iceland and ending in the Southern Ocean at approximately 60°S. A16N is principally along 20°W and A16S is principally along 25°W. These cruises are part of a decadal series of repeat hydrography sections jointly funded by the NOAA Climate Program Office and the National Science Foundation Division of Ocean Sciences as part of the Climate Variability and Predictability Study (CLIVAR) CO_2 Repeat Hydrography Program, which was updated in 2007 to the Global Ocean Ship-based Hydrographic Investigations Program (GO-SHIP). The repeat hydrography program focuses on the need to monitor inventories of CO_2, heat and freshwater and their transports in the ocean. Earlier programs under WOCE, JGOFS, and CLIVAR have provided baseline observational fields for these parameters. The new measurements will reveal much about the changing patterns on decadal scales. The program serves as a structure for assessing changes in the ocean's biogeochemical cycle in response to natural and/or human-induced activity.

The NOAA ship R/V *Ronald H. Brown* departed Reykjavik, Iceland on the 3rd August 2013, after a short two day delay. The ship proceeded south principally along a 20°W cruise track, previously measured in 1988/89, 1991/93 and 2003/05, conducting a full-depth CTD/rosette/LADCP cast approximately every 0.5°. At ~35°N the track turned west diagonally crudely mirroring the coast of North Africa. The first leg of A16N ended on 23rd August 2013 in Funchal, Madeira (Portugal). After a short delay for ship repairs the second leg departed on 9th September 2013 continuing south around Africa, reaching 25°W at approximately 3.5°N and continuing straight south. The 2nd leg ended on 3rd October in Natal, Brazil after delays to divert around Hurricane Humberto and the loss of the CTD package. The A16S cruise departed Recife, Brazil on 23rd of December after a two day delay waiting for a new CTD wire. The ship reoccupied the last station of A16N and then continued south along 25°W, the ship then turned west at around 35.5°S to complete a diagonal towards South Georgia Island, then headed diagonally East, reaching the final station at 60°S, 31°W. The cruise ended on 4th February, 2014 in Punta Arenas, Chile. The full cruise track is shown in the figure on the cover. Underway measurements of surface seawater (temperature, salinity, pCO_2, ADCP) and atmospheric measurements (pCO_2, CFCs, aerosols) were also made along the cruise track. The complete coordinates of the waypoints can be found in Appendix A.

Fifty-five scientists from 14 academic institutions and three NOAA research facilities participated in this cruise (Appendix B). Our group measured total alkalinity (TA), total CO_2 (TCO_2) and pH by potentiometry and pH by spectrophotometry. The final dataset for all measured parameters is freely available at the Carbon Dioxide Information Analysis Center (CDIAC) (http://cdiac.ornl.gov/oceans/RepeatSections/). Only the total alkalinity and spec pH are reported to CDIAC.

2. Description of Variables and Methods

Total alkalinity and pH are the main variables determined by our group. The use of a closed cell titration allows us to also determine the TCO_2 and pH by potentiometry which provides a check on our systems, these values are not reported to

CDIAC since this method provides lower precision than other methods used on the cruise. A detailed description of the methods is found below.

2.1 Total Alkalinity Analyses

Total alkalinity can be conceptually thought of as the sum of the excess bases in seawater, principally carbonate and bicarbonate, with small contributions from borate and other bases. The standard method for determination is through potentiometric titration with hydrochloric acid. Details of the sampling collection and analysis are given below.

2.1.1 Sampling:

Samples for total alkalinity were drawn from the 10 L niskin bottles into 500 cm^3 borosilicate bottles using silicone tubing that fit over the petcock. This tubing both helped avoid contaminating dissolved organic carbon (DOC) samples and allowed samples to be filled from the bottom, entraining little to no bubbles. Bottles were rinsed a minimum of two times and filled from the bottom, overflowing at least half of the volume. Approximately 15 cm^3 of water was withdrawn from the flask by arresting the sample flow and removing the sampling tube, thus creating a small expansion volume and a reproducible headspace. The sample bottles were sealed at a ground glass joint with a glass stopper. The samples were thermostated at 25°C before analysis. At most stations, duplicate samples were taken near the surface, the bottom, and the oxygen minimum layer.

2.1.2 Analyzer Description:

The total alkalinity of seawater was evaluated from the proton balance at the alkalinity equivalence point, pH_{equiv} = 4.5 at 25ºC in one kilogram of sample. The method utilizes a multi-point hydrochloric acid titration of seawater according to the definition of total alkalinity (Dickson, 1981). The potentiometric titrations of seawater using a closed cell give values of TA, Dissolved Inorganic Carbon (DIC or TCO_2) and pH, which is determined from the initial EMF.

Two titration systems, A and B, were used for measuring TA. Each system used a Metrohm 665 or 765 Dosimat titrator, an Orion 720A pH meter and a custom designed plexiglass water-jacketed closed titration cell (Millero *et al*., 1993b). The seawater samples were equilibrated to a constant temperature of 25 ± 0.1ºC with a water bath (Neslab, model RTE-10 or RTE-17). The water-jacketed cell has a volume of ~200 cm^3. Each cell has a fill and drain valve that is electronically activated to increase the reproducibility of the volume of sample. A typical titration recorded the EMF after the readings became stable (deviation less than 0.09 mV) and then enough acid was added to change the voltage a pre-assigned increment (13 mV). A full titration (~25 points) takes about 20 minutes. The electrodes used to measure the EMF of the sample consisted of a ROSS glass pH electrode (Orion, model 810100) and a double junction Ag, AgCl reference electrode (Orion, model 900200).

An integrated program controls the titration, data collection, and the calculation of the carbonate parameters (TA, pH, and TCO_2) (Millero *et al.*, 1993a). The program is patterned after those developed by Dickson (1981), Johansson and Wedborg (1982), and Dickson et al. (2007). The program uses a Levenberg-

Marquardt nonlinear least-squares algorithm to calculate E^0, pH, TA, TCO_2 and pK^*_1 from the potentiometric titration data. A diagram of the system is shown in Appendix C.

2.1.3 Reagents:

A single 50 L batch of ~0.25 m HCl acid was prepared in 0.45 m NaCl by dilution of concentrated HCl, AR Select, Mallinckrodt, to yield a total ionic strength similar to seawater of salinity 35.0 (I = 0.7 M). The acid was standardized by a coulometric technique (Marinenko and Taylor, 1968; Taylor and Smith, 1959), and verified with alkalinity titrations on certified reference material (CRM). The calibrated normality of the acid used was 0.24361 ± 0.0001 N HCl. The acid was stored in 500-ml glass bottles sealed with Apiezon® M grease for use at sea.

2.1.4 Standardization:

The volumes of the cells used were calibrated to ± 0.03 cm^3 in port in Reykjavik, Madeira, and Recife before the start of each leg by multiple titrations using Certified Reference Material (CRM) provided by Dr. Andrew Dickson, Marine Physical Laboratory, La Jolla, California. The certified values for the batches used are given in **Table 1**. Calibrations of the burette of the Dosimat with water at 25ºC indicate that the systems deliver 3.000 cm^3 (the approximate value for a titration of seawater) to a precision of ± 0.0004 cm^3, resulting in an error of ± 0.3 $\mu mol \cdot kg^{-1}$ in TA. The reproducibility and precision of measurements are checked using low nutrient surface seawater collected from the ship's flowing seawater system and CRMs. CRMs were utilized in order to account for instrument drift and to maintain measurement precision. Duplicate analyses provide additional quality assurance and were taken from the same Niskin bottle. Duplicates were either measured on the same instrument, A or B, or measured one on each system.

Table 1. The assigned values of CRM batches 114 and 129 provided by A. Dickson of SIO

Batch 114	
Parameter	***Assigned Value***
Salinity	33.208
Total Alkalinity	2217.91 ± 0.68 $\mu mol \cdot kg^{-1}$
Total Dissolved Inorganic Carbon	2000.93 ± 0.44 $\mu mol \cdot kg^{-1}$
Phosphate	0.36 $\mu mol \cdot kg^{-1}$
Silicate	2.4 $\mu mol \cdot kg^{-1}$
Nitrite	0.00 $\mu mol \cdot kg^{-1}$
Nitrate	0.97 $\mu mol \cdot kg^{-1}$
Batch 129	
Parameter	***Assigned Value***
Salinity	33.361
Total Alkalinity	2237.32 ± 0.52 $\mu mol \cdot kg^{-1}$
Total Dissolved Inorganic Carbon	2016.65 ± 0.32 $\mu mol \cdot kg^{-1}$
Phosphate	0.34 $\mu mol \cdot kg^{-1}$
Silicate	4.1 $\mu mol \cdot kg^{-1}$
Nitrite	0.00 $\mu mol \cdot kg^{-1}$
Nitrate	0.83 $\mu mol \cdot kg^{-1}$

2.2 Discrete pH Analyses

The pH is measured using an indicator dye and a spectrophotometer. In seawater there are several different definitions or scales for pH which complicates the measurement. The three main scales used are the free scale (pH_F) which only includes the concentration of the free proton ($[H^+]_F$), the total scale (pH_T) defined as:

$$pH_T = [H^+]_F + [HSO_4^-] \quad (1)$$

and the seawater scale:

$$pH_{sws} = [H^+]_F + [HSO_4^-] + [HF] \quad (2)$$

The subscripts F, T, and SWS are used to distinguish between the different scales. All values reported here are on the seawater scale unless mentioned otherwise.

2.2.1 Sampling:

At each station samples were drawn directly from the niskin bottles on the rosette into 50 cm^3 glass syringes using polycarbonate Luer-lock 3-way valves that fit directly on the petcock of the niskin bottle. The syringes were rinsed a minimum of two times and filled while taking care not to entrain any bubbles. After collection the syringe was checked for bubbles and any found were ejected. The samples were thermostated at 25°C before analysis.

2.2.2 Analyzer Description:

Measurements of the pH of seawater, on the total scale (pH_T) were first made using multi-wavelength spectrophotometric techniques and equations of Clayton and Byrne (1993) which was calibrated using TRIS buffers (Ramette et al., 1977). The values were then converted to the seawater scale (pH_{sw}) using the dissociation constants of H_2SO_4 (Dickson, 1990) and HF (Dickson and Riley, 1979). The Sulphonphthalein indicator m-cresol purple (mCp) was used to make the pH measurements using the methods of Clayton and Byrne (1993) as modified by Lee et al. (1996). The system is patterned after the standard operating procedure developed by the U.S. Department of Energy (DOE) (Dickson et al., 2007). The automated system performs discrete analysis of pH on samples approximately every 6 minutes using a total of 40 cm^3 of sample. The syringes are stored in a water bath at 25°C to maintain a constant temperature. A refrigerated circulating temperature bath (Neslab, model RTE-10) regulates the temperature of the sample at 25 ± 0.05ºC. A microprocessor controlled syringe pump (Kloehn V6) with a 10 cm^3 syringe and sampling valve aspirates and injects the seawater sample into the 10 cm micro-volume optical cell (Starna Cells, Inc.) at a precisely controlled rate. The syringe pump rinses and primes the optical cell with 20 cm^3 of sample and the software permits 90 seconds for temperature stabilization. An Agilent 8453 UV/VIS spectrophotometer measures background absorbance of the sample. The automated syringe pump and sampling valves aspirates 9.90 cm^3 seawater and 0.10 cm^3 of indicator and injects the mixture into the cell. After the software permits 90 seconds for temperature stabilization, a Guildline 9540 digital platinum resistance thermometer measures the temperature and the spectrophotometer acquires the absorbance at 434, 578, 730, and 488 nm. The full spectra from 190-900 nm at 1 nm intervals are also archived. A diagram of the system is shown in appendix D.

A one liter batch of mCp indicator was used for all three legs. Unpurified indicator from Sigma-Aldrich lot number 87H3629 was used. Since unpurified indicator was used the updated equations of Liu et al. (2011) were NOT used, and instead the values were corrected using the indicator correction.

The addition of indicator slightly perturbs the pH of the sample. To account for this an indicator correction must be made. This is done by making additional measurements on a subset of the samples (approximately 1 per station), in which the sample is measured a second time using twice the amount of indicator. It was insured that the entire pH range was adequately covered over the course of the cruises. The change in the absorbance ratio (ΔR) was then determined by fitting the measurements to the following equation:

$$\Delta R = A + BR \tag{3}$$

Where R is the absorbance ratio from a single addition of indicator. The corrected absorbance ratio (R_{corr}) is then calculated using:

$$R_{corr} = R + (A + BR) * (A_{488}-A_{730}) \tag{4}$$

The absorbance at the isosbestic point (488 nm) is used instead of the volume of the indicator as was done by Clayton and Byrne (1993) because it is more precise than assuming a constant volume of indicator is added. For A16N the value of A = -0.0609 and B = 0.0517. For A16S the value of A = -0.0621 and B = 0.0457.

3. Accuracy and Precision of Measurements

The accuracy and precision of both measurements was checked using several different methods. For total alkalinity certified reference material (CRMs) were used to determine accuracy. For pH there is no certified standard, but CRMs were also measured and compared to the values calculated from the certified TA and TCO_2. The precision of the total alkalinity was checked using low nutrient surface seawater collected in 20 L batches as needed from the ship's flowing seawater system. A TRIS buffer was used to check the precision of the pH samples. For both total alkalinity and pH duplicates were also measured on each station to check precision. Details of the results are given in the following sections.

3.1 Total Alkalinity Accuracy and Precision

Several methods were used to determine the accuracy and precision of the total alkalinity measurements. A comparison of measured values of TA, TCO_2, and pH made on CRMs during the cruise are given in **Table 2**. The differences between the measured values of TA, TCO_2 and pH are shown in **Figures 1 to 3.** Values of TCO_2 and pH from bottles obtained from the DIC group after their analysis are not reported due to probable loss of CO_2 after opening. This includes all bottles from batch 114 and some bottles from batch 129. There is a distinct jump in the ΔTA on system A during A16S, this is the result of a repair made to the top valve and level sensor causing a small change in the cell volume.

The precision in the measured values of TA, TCO_2 and pH are reasonable. The average measured value for TA is in good agreement with the assigned value. The measured values of TCO_2 are higher than the assigned value as found in previous studies (Millero et al. 1993b). The CRM values are slightly higher on the south cruise, compared to the north. The station data have been corrected to the CRM values using the ratio of the certified value to measured value. The average correction for TA is less than 2 $\mu mol \cdot kg^{-1}$, with a maximum correction of 3.5 $\mu mol \cdot kg^{-1}$.

Table 2. Comparison of the measured TA ($\mu mol \cdot kg^{-1}$), TCO_2 ($\mu mol \cdot kg^{-1}$), and pH with the values of CRM from Cell A and B during the cruise. CRM is the certified value.

A16 North					
Batch 129, Cell A					
Parameter	***CRM***	***Average***	***Stdev***	***Number***	***Meas - CRM***
TA	2237.32	2236.21	1.96	47	-1.11
TCO_2	2016.65	2022.87	2.73	46	6.22
pH	7.9122[a]	7.899	0.006	46	-0.013
Batch 114, Cell A					
TA	2217.91	2217.52	1.92	19	-0.39
Batch 129, Cell B					
TA	2237.32	2237.85	2.44	52	0.53
TCO_2	2016.65	2027.51	3.88	51	10.86
pH	7.9122[a]	7.895	0.006	48	-0.017
Batch 114, Cell B					
TA	2217.91	2220.22	2.87	16	2.31

A16 South					
Batch 129, Cell A					
Parameter	***CRM***	***Average***	***Stdev***	***Number***	***Meas - CRM***
TA	2237.32	2239.17	1.99	42	1.85
TCO_2	2016.65	2030.81	1.55	25	14.16
pH	7.9125[a]	7.895	0.002	25	-0.018
Batch 129, Cell B					
TA	2237.32	2240.32	2.40	43	3.00
TCO_2	2016.65	2032.56	3.23	24	15.91
pH	7.9125[a]	7.896	0.010	24	-0.017

a) This value of pH is calculated from an input of TA and TCO_2 assigned the CRM in CO_2Sys and is not a certified value.

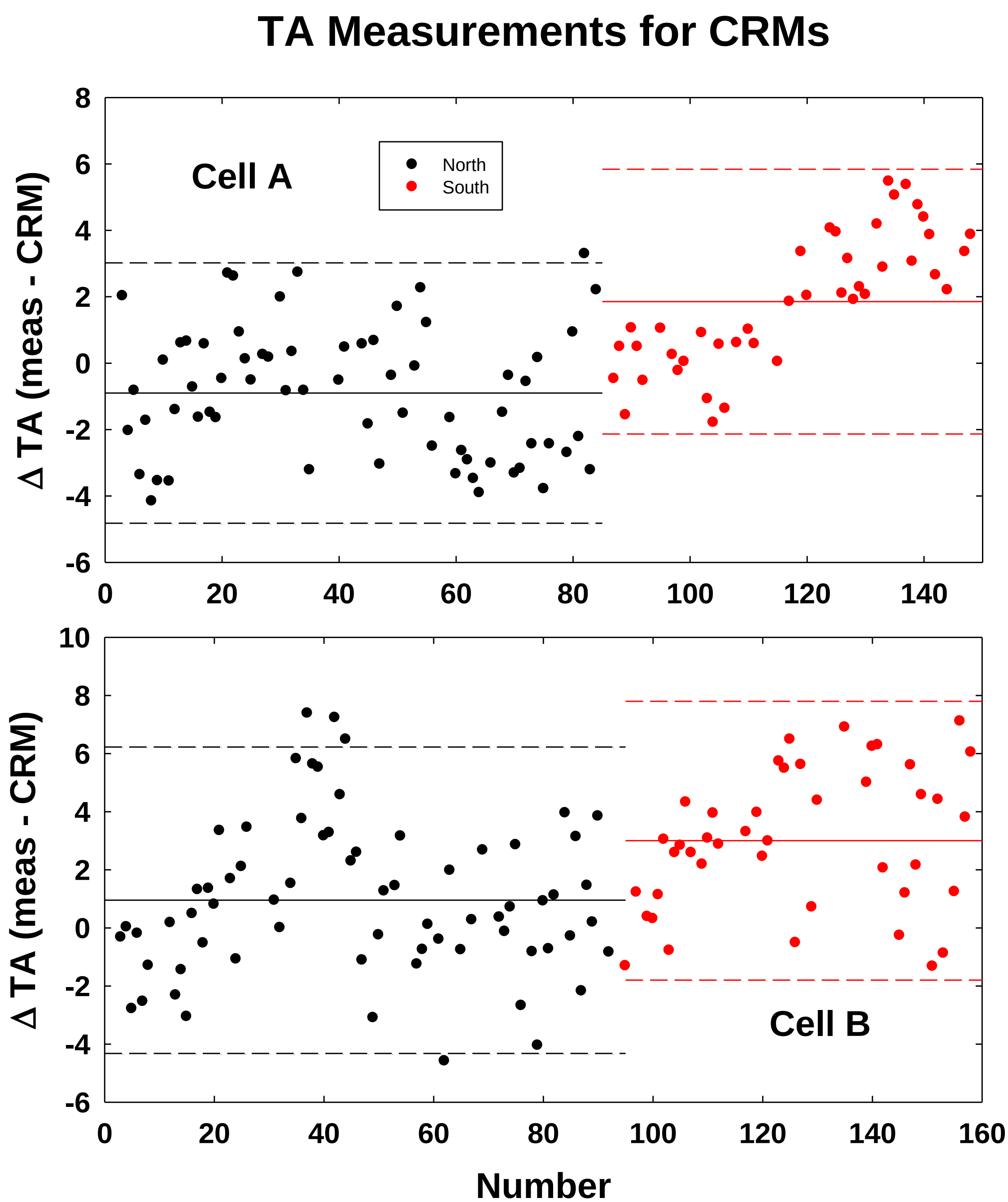

Figure 1. **The difference between the measured TA ($\mu mol \cdot kg^{-1}$) with the certified values of 2237.32 and 2217.91 $\mu mol \cdot kg^{-1}$ (batches 129 and 114 respectively). The standard deviations are ± 1.95 and ± 1.99 $\mu mol \cdot kg^{-1}$, respectively for the north and south in cell A, and ± 2.54 and ± 2.40 $\mu mol \cdot kg^{-1}$, respectively for the north and south in cell B. The dashed lines are the 2 standard deviation boundaries from the means (solid lines). The large jump in cell A during the south leg corresponds to a repair made on the cell.**

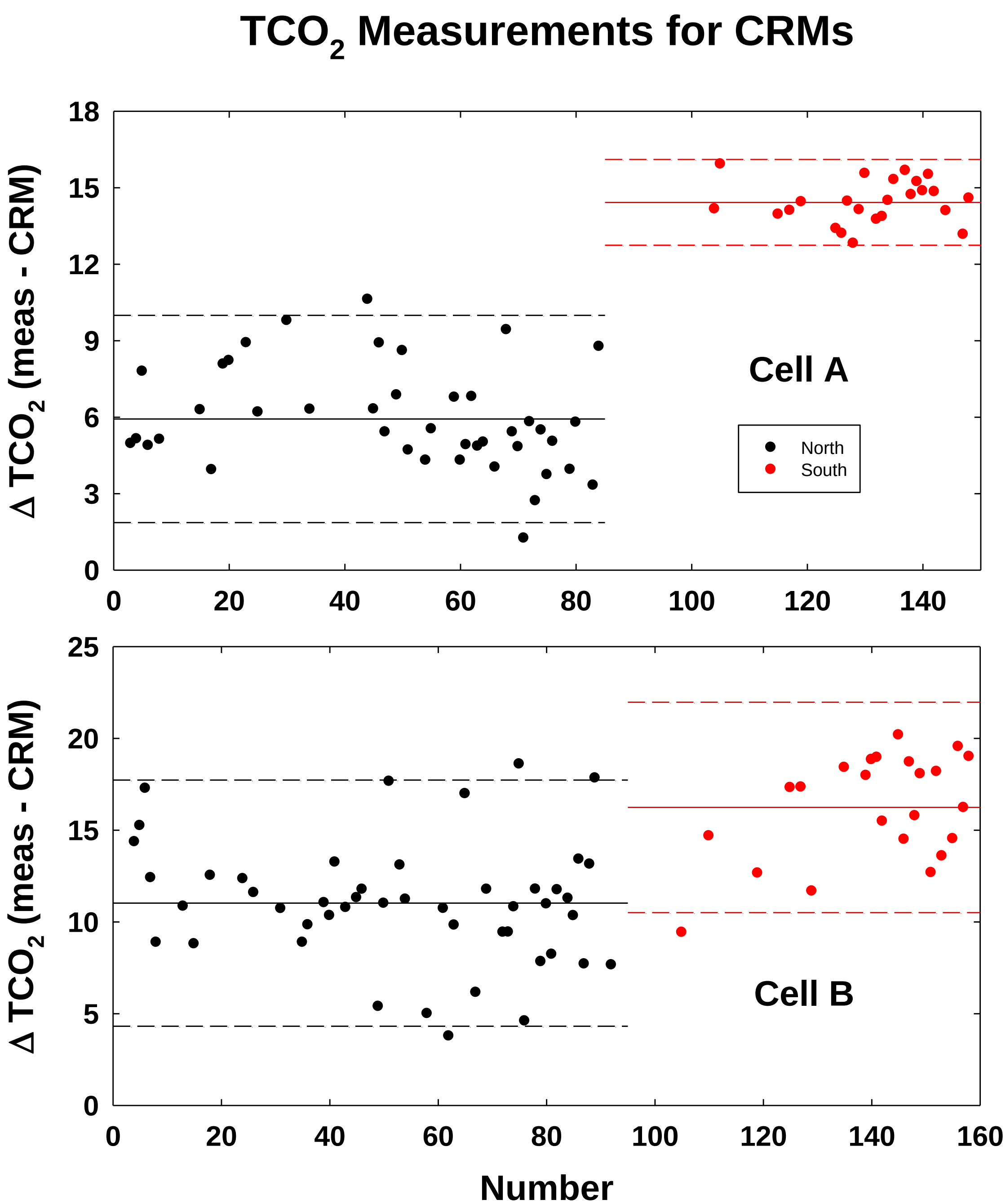

Figure 2. The difference between the measured TCO_2 ($\mu mol \cdot kg^{-1}$) with the certified reference value of 2016.65 (batch 129). The standard deviations are ± 2.73 and ± 1.55 $\mu mol \cdot kg^{-1}$, respectively for the north and south in cell A, and ± 3.88 and ± 3.23 $\mu mol \cdot kg^{-1}$, respectively for the north and south in cell B. The dashed lines are the 2 standard deviation boundaries from the means (solid lines).

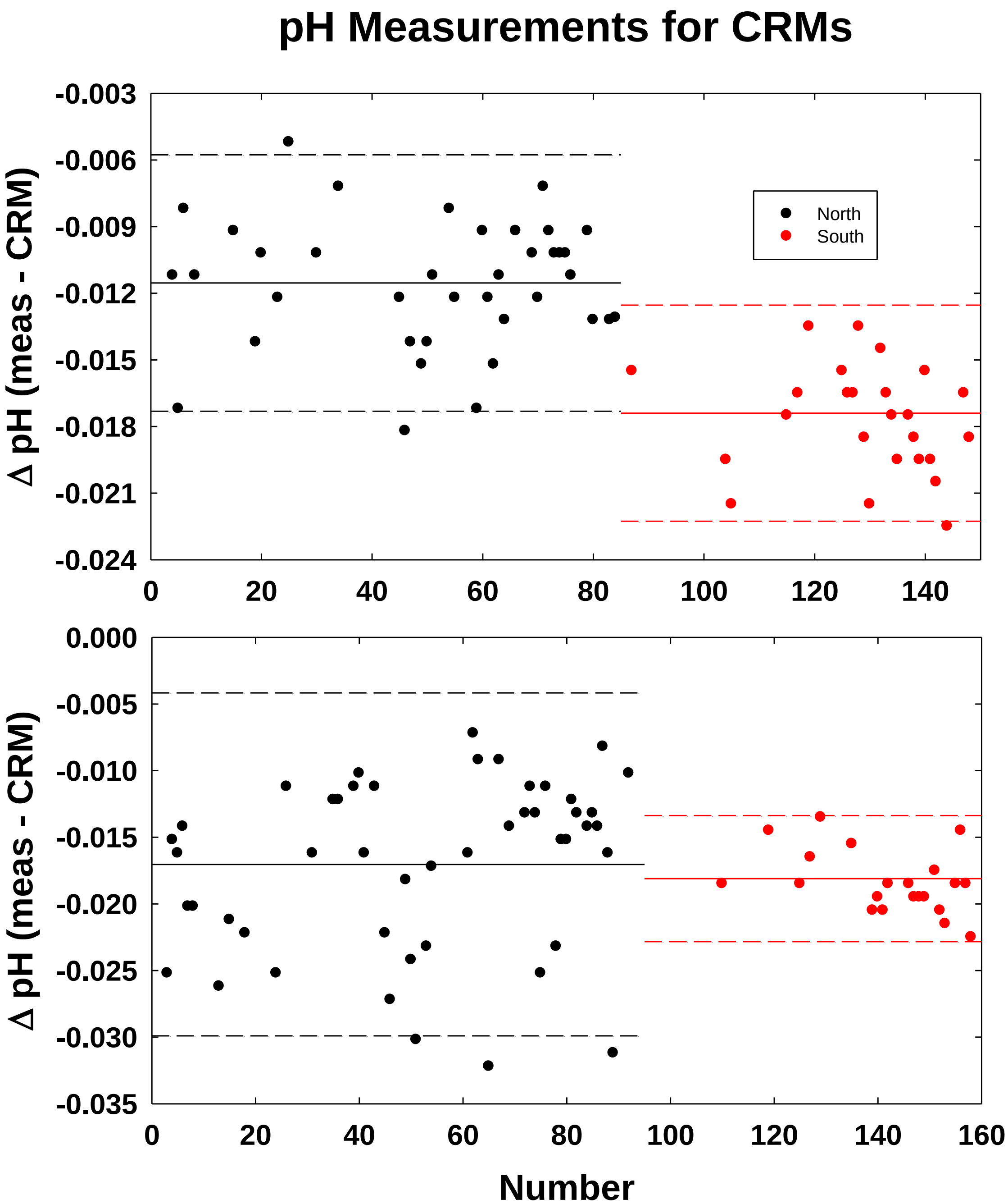

Figure 3. The differences between the measured potentiometric pH and calculated values of pH = 7.9122 for the north and pH = 7.9125 for the south (batch 129). The standard deviations are ± 0.0063 and ± 0.0024 µmol·kg^{-1}, respectively for the north and south in cell A, and ± 0.0064 and ± 0.0099 µmol·kg^{-1}, respectively for the north and south in cell B. The dashed lines are the 2 standard deviation boundaries from the means (solid lines).

Although the potentiometric values of pH are precise, For A16N the offset in A and B was 0.012 and 0.017 respectively and for A16S it was 0.017 and 0.018 respectively. This has been found in earlier studies and is probably related to the non-Nernstian behavior of the electrodes or absorption of atmospheric CO_2 that decreases the pH without affecting the total alkalinity. Thus, an adjustment was made to all potentiometric pH values by calibrating the cell with known CRM pH values calculated from the TA and TCO_2 CRM values. The average difference between the titration pH and the CRM value (**Figure 3**) we used to correct for the potentiometric pH measurements of the samples.

A total of 12 batches of low nutrient surface seawater were used on A16N. The precision (standard deviation) was typically ~2 $\mu mol \cdot kg^{-1}$, with a standard deviation of less than one for several batches. On A16S a total of 6 batches were used, and had similar precision as the northern legs.

The reproducibility of the measurements was also checked by comparing the results of both systems on seawater sampled from the same Niskin bottle. The results of measurements for the same samples on both systems (cells A and B) are given in **Table 3** and **Figure 4**. The measurements of TA with the same sample on both cells normally agreed to less than ± 3 $\mu mol \cdot kg^{-1}$, while TCO_2 was slightly higher at less than ± 3.5 $\mu mol \cdot kg^{-1}$. The values of pH agreed to about ± 0.005.

Duplicate measurements were also made on the same system. The results are given in **Table 4** and **Figures 5 and 6**. The reproducibility of both systems are in good agreement (standard deviation of ~ ± 2 μmol·kg^{-1} or less for TA and TCO_2 and ± 0.003 for pH). These are typical precisions for at sea measurements using this method.

Table 3. Comparison of measurements of TA, TCO_2 and pH of the same sample on the two systems.

		System A – System B	
		North	**South**
TA (μmol·kg^{-1})	Mean	0.27	-1.22
	Stdev	2.38	2.74
	N	92	98
TCO_2 (μmol·kg^{-1})	Mean	-4.17	-2.47
	Stdev	2.73	3.40
	N	92	93
pH	Mean	0.005	0.002
	Stdev	0.004	0.005
	N	91	90

Table 4. Comparison of duplicate measurements of TA (μmol·kg^{-1}), TCO_2 (μmol·kg^{-1}) and pH on the same system.

		North			*South*	
		System A	**System B**		**System A**	**System B**
TA (μmol·kg^{-1})	Mean	0.43	-0.12	Mean	0.04	-0.08
	Stdev	1.14	2.29	Stdev	1.84	1.69
	N	117	107	N	103	92
TCO_2 (μmol·kg^{-1})	Mean	0.58	-0.10	Mean	0.31	0.21
	Stdev	1.14	1.60	Stdev	0.88	1.86
	N	114	101	N	95	91
pH	Mean	-0.0003	-0.0002	Mean	-0.0003	-0.0006
	Stdev	0.0022	0.0027	Stdev	0.0026	0.0028
	N	111	100	N	98	89

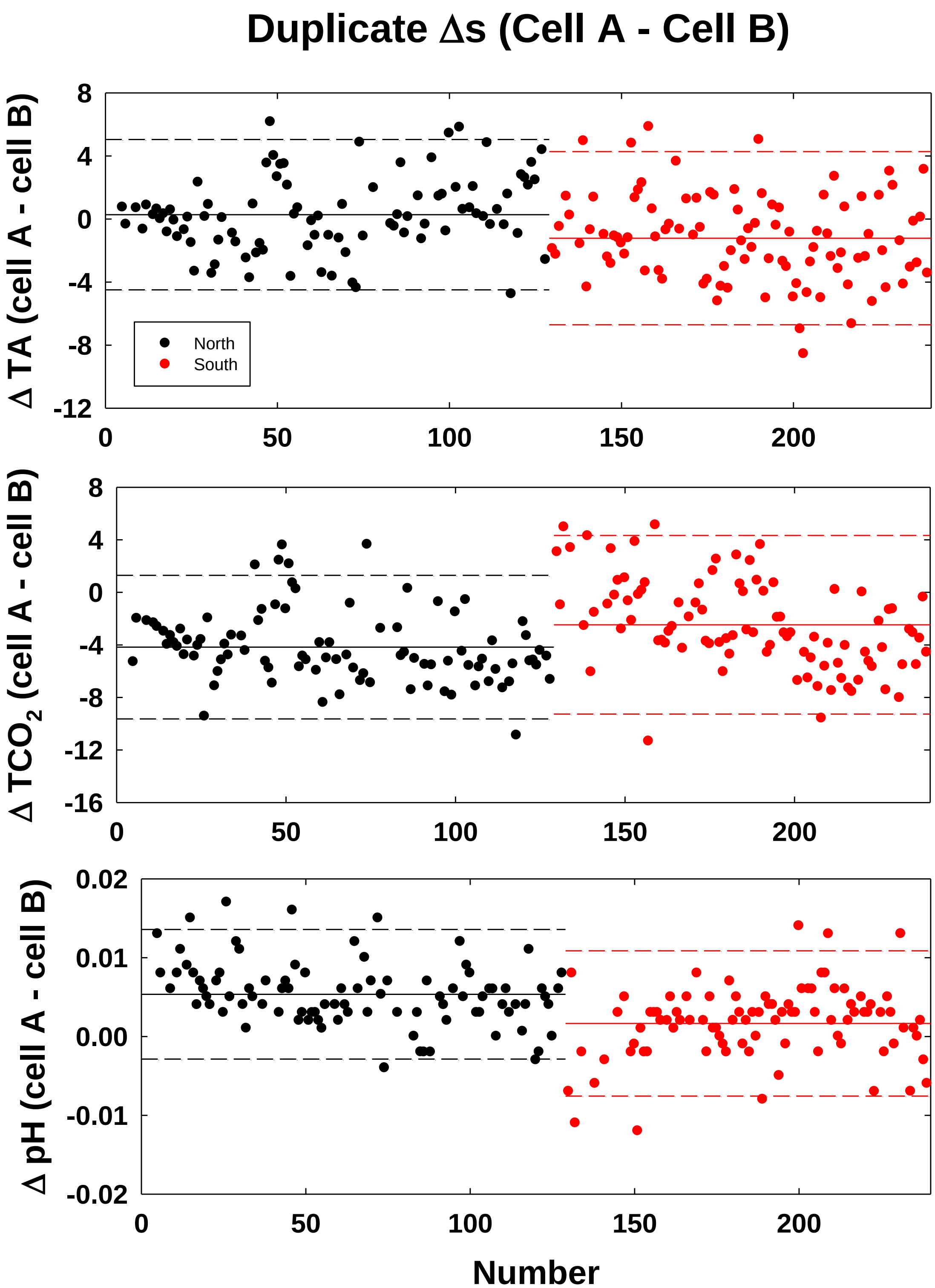

Figure 4. Precision of TA (µmol·kg^{-1}), TCO_2 (µmol·kg^{-1}) and pH measurements between cells A and B. The dashed lines are the 2 standard deviation boundaries from the means (solid lines).

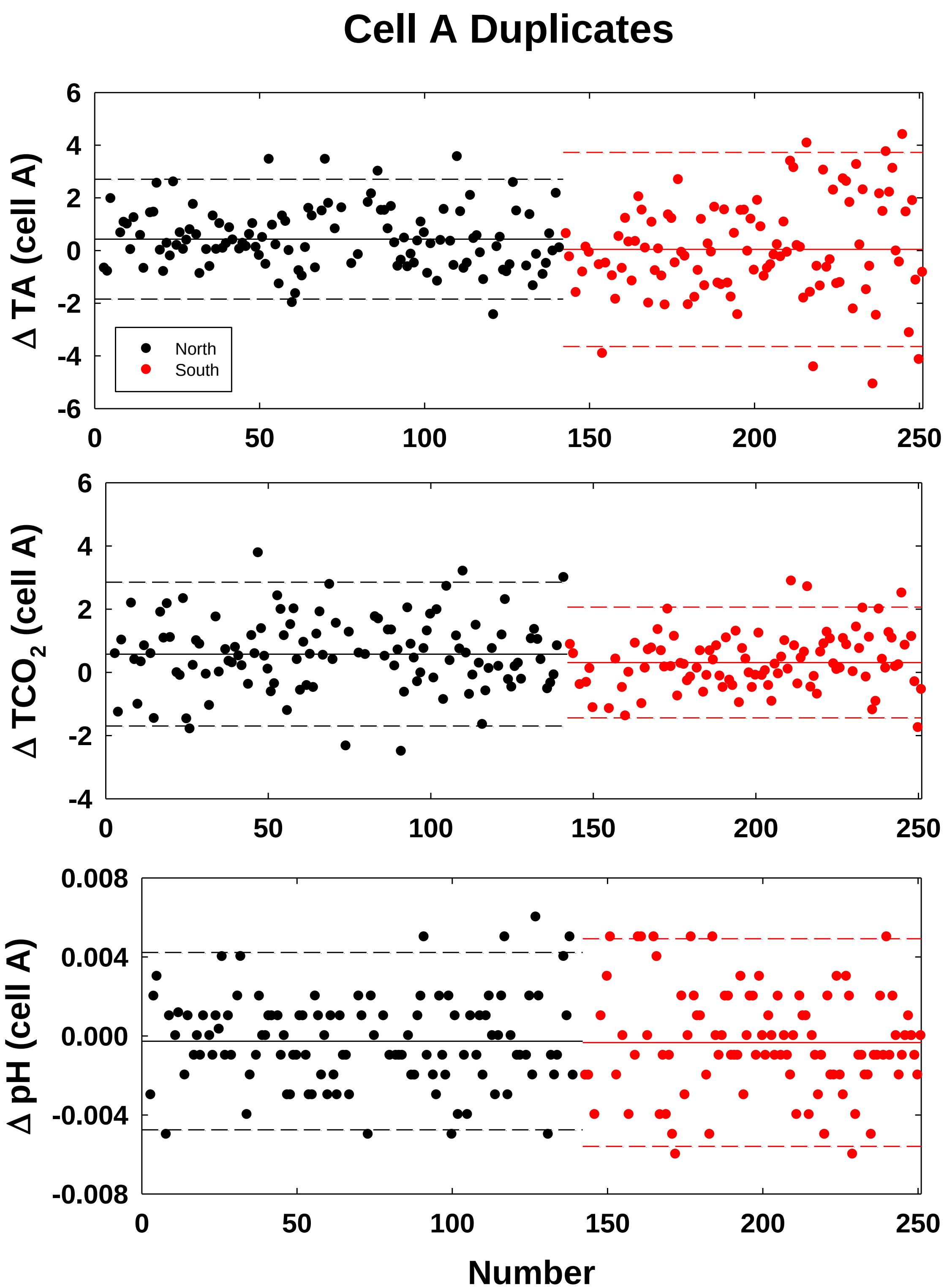

Figure 5. The reproducibility of TA (μmol·kg^{-1}), TCO_2 (μmol·kg^{-1}) and pH on cell A. The dashed lines are the 2 standard deviation boundaries from the means (solid lines).

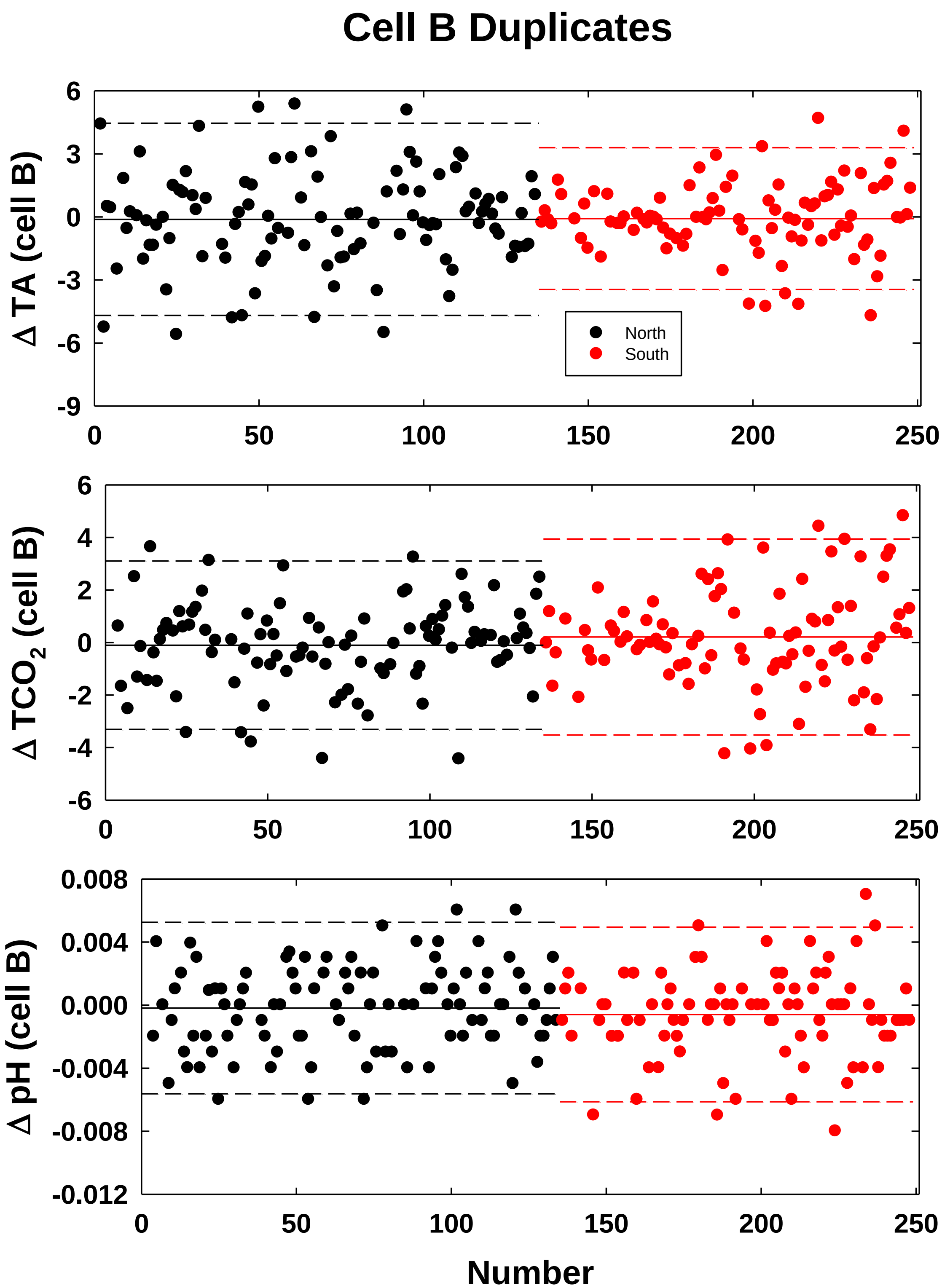

Figure 6. The reproducibility of TA (μmol·kg⁻¹), TCO_2 (μmol·kg⁻¹) and pH on cell B. The dashed lines are the 2 standard deviation boundaries from the means (solid lines).

The NOAA AOML group also measured TCO_2 using the more precise SOMMA method, which uses coulometry. The difference in the corrected potentiometric values of TCO_2 with the values determined by SOMMA is shown in **Figure 7**. The mean difference is -4.5 ± 4.1 $\mu mol \cdot kg^{-1}$ (N = 2828) for the northern portion of the cruise and -8.4 ± 4.1 $\mu mol \cdot kg^{-1}$ (N = 2445) for the southern portion.

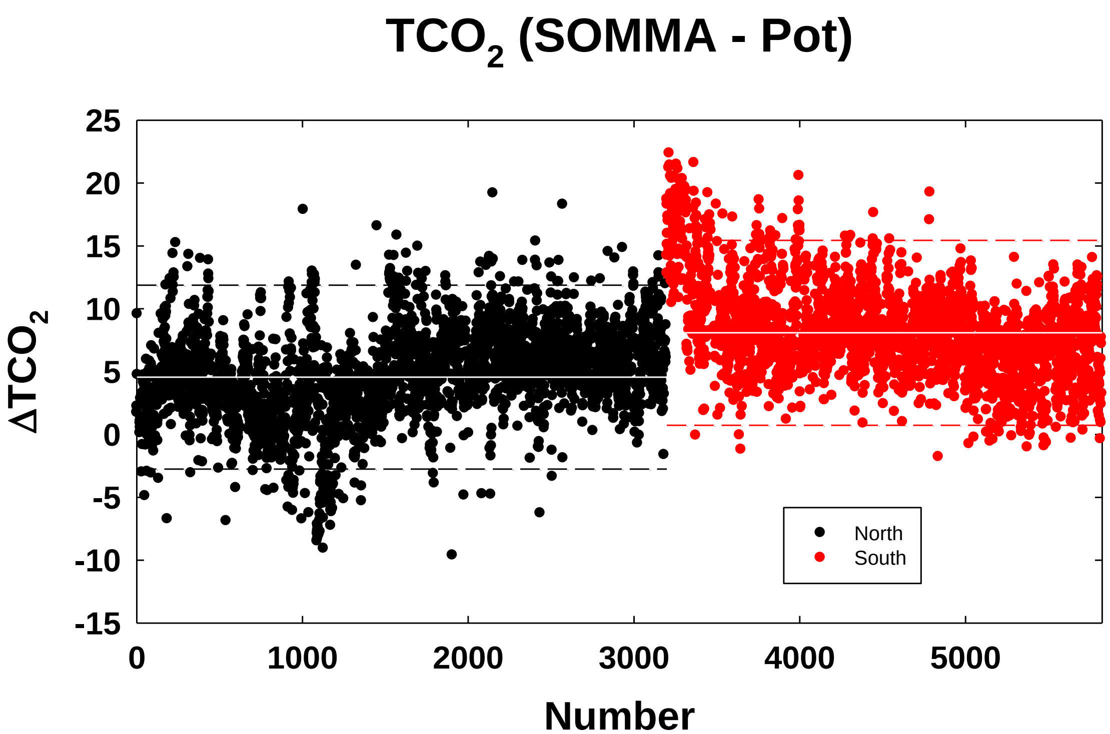

Figure 7. Difference between the TCO_2 ($\mu mol \cdot kg^{-1}$) measured by SOMMA and potentiometry. The dashed lines are the 2 standard deviation boundaries from the means (white lines).

3.2 Discrete pH Accuracy and Precsion

The reproducibility of the spectrophotometric pH system was monitored throughout the cruise by making measurements on CRM, TRIS buffer, and duplicates of the same sample. The results of the CRMs and TRIS buffer are given in **Table 5** and the results of duplicate measurements are given in **Table 6** and are shown in **Figure 8**.

Table 5. Accuracy and precision of spectrophotometric pH measurements using CRM and TRIS buffer.

	North	***South***
CRM	7.9115 ± 0.0032 n = 61	7.9111 ± 0.0030 n = 49
ΔCRM	-0.0007 ± 0.0032 n = 61	-0.0014 ± 0.0030 n = 49
TRIS[a]	8.0888 ± 0.0037 n = 63	8.0890 ± 0.0032 n = 39

a. The TRIS does not include any Fluoride so value is reported on the total scale

An 8 L batch of TRIS buffer was prepared in the lab before the cruise according to the recipe of Millero et al. 1993a. This does not include any fluoride so values are reported on the total scale. The TRIS was stored in 500 cm^3 borosilicate bottles sealed with ground glass stoppers and Apiezon® M grease. Something started growing in the TRIS bottles in between the first and second leg of the North section. Any affect this may have on the measurements appears to be small since there is no significant difference between the first and second leg and the values measured on the cruise are in reasonable agreement with measurements made in the lab before the cruises (8.0897 ± 0.0017, N=9). The standard deviation is also comparable to the CRMs. On the South leg TRIS bottles 6 and 7 were about 0.016 higher than all other bottles, possibly because of the organism growing in the bottles. These values have been excluded from the results.

Table 6. Precision of spectrophotometric pH measurements using duplicates

	North	*South*
ΔDuplicates	-0.0006 ± 0.0017 n = 244	0.0004 ± 0.0018 n = 197

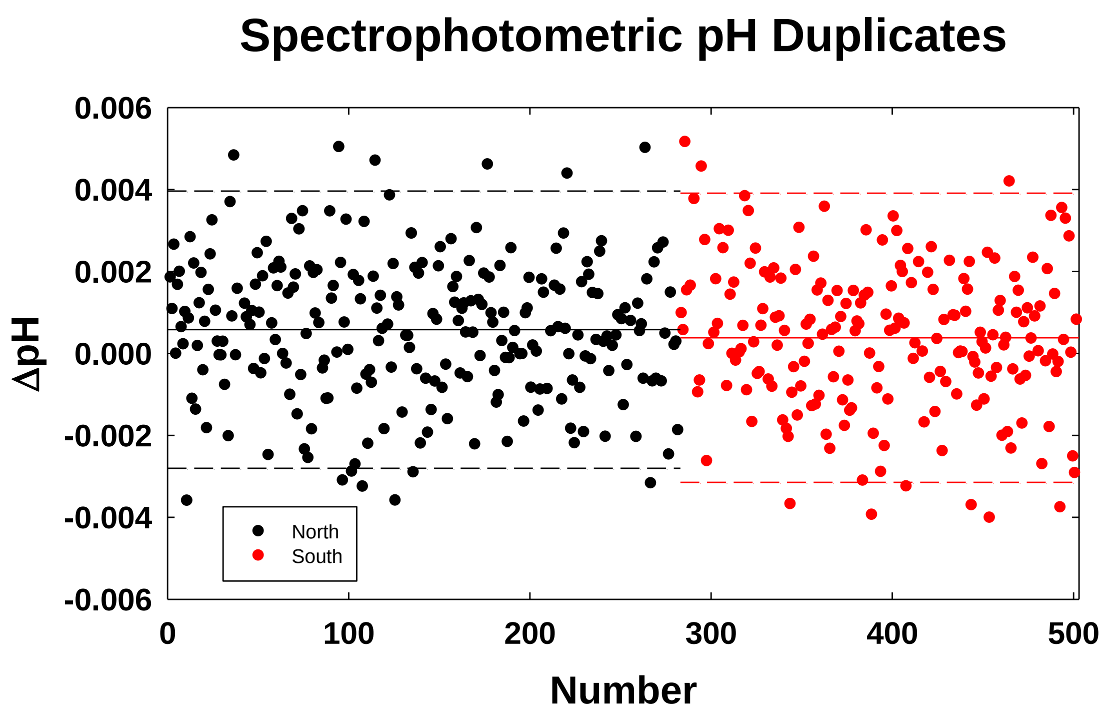

Figure 8. Precision of spectrophotometric pH measurements using duplicates. The dashed lines are the 2 standard deviation boundaries from the means (solid lines).

The values obtained by the two different methods (spec and potentiometric) were compared. The differences in the corrected potentiometric values of pH with the values determined by spectrophotometry are shown in **Figure 9**. The mean difference is 0.006 ± 0.0057 (N = 2649) for the northern portion of the cruise and 0.011 ± 0.0048 (N = 2344) for the southern portion.

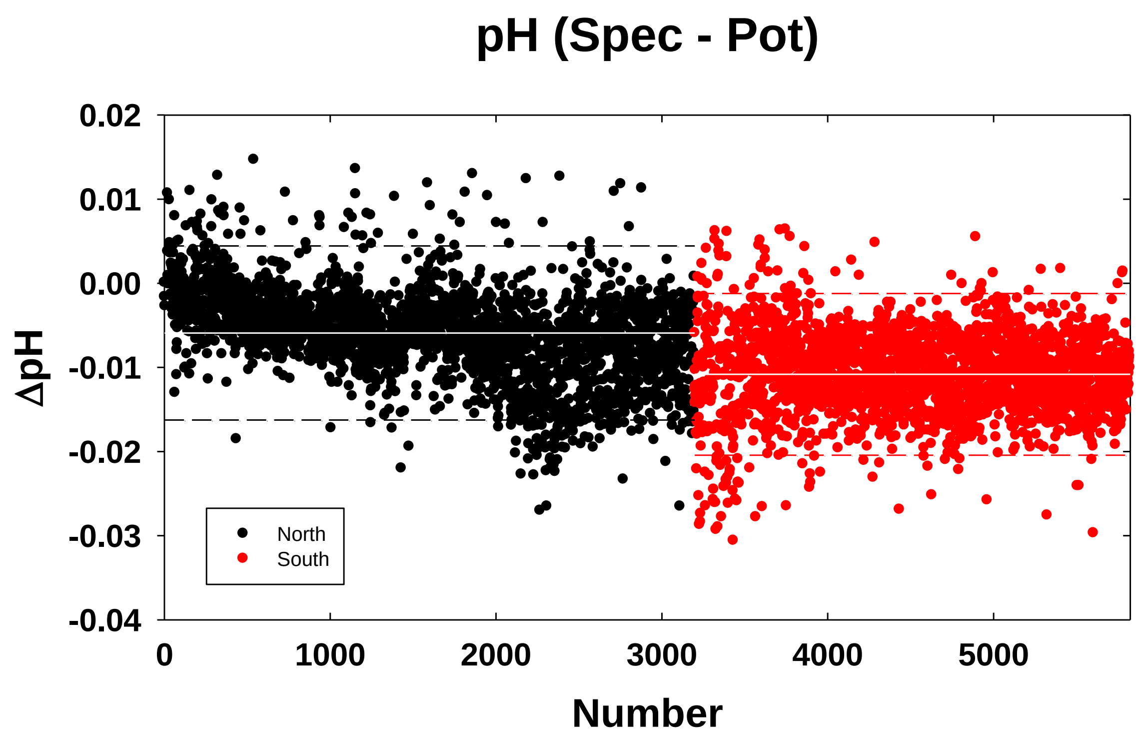

Figure 9. Difference between the pH measured by spectrophotometry and potentiometry. The dashed lines are the 2 standard deviation boundaries from the means (white lines).

4. Internal Consistency

The carbonate system is characterized by four parameters: total alkalinity, total carbon dioxide, partial pressure of carbon dioxide (pCO_2) and pH. Knowing two of these parameters, one can calculate the other two. If more than two parameters are known, a comparison of calculated and measured values can be used to examine the internal consistency of the system. We have examined the internal consistency of our pH and TA measurements with the SOMMA values of TCO_2 and the discrete pCO_2 values measured by AOML. The SOMMA and pCO_2 data are the preliminary results submitted at the end of the cruise and not the final data. We used the Excel version

2.1 of CO_2sys program (Pierrot et al. 2006) using the carbonic acid constants of Millero (2006) and Borate concentrations of Lee et al. (2010) for all calculations.

Since all four parameters were measured on this cruise all 12 possible combinations were calculated. The results of these calculations are summarized in **Table 6** and the deviations are shown in **Figure 10-13**. Excluding inputs of (pH,pCO_2), the calculated values of ΔTA and ΔTCO_2 are all reasonable with standard deviations below ± 5 $\mu mol \cdot kg^{-1}$. The calculated values of ΔpH are similarly reasonable and all show standard deviations below ± 0.01. The calculated values of ΔpCO_2 show large offsets and standard deviations. Low pCO_2 values are internally consistent, but large offsets appear at high concentrations. This trend has been found before (Hoppe et al. 2012), although the exact cause is currently unknown. **Figure 14** illustrates this using data from A16N, all other pCO_2 calculations show similar trends. There is also much larger scatter in the pCO_2 data for the second leg of A16N than either the first leg or A16S.

Table 7. Difference between the measured and calculated values of TA, pH, TCO_2, and pCO_2.

A16 North				
Parameter	**Input**	**Mean**	**Stdev**	**Number**
ΔTA	pH, TCO_2	-2.58	4.53	2658
	TCO_2, pCO_2	-5.73	4.81	2045
	pCO_2, pH	37.81	51.32	1948
ΔTCO_2	TA, pH	2.39	4.23	2658
	pH, pCO_2	39.64	46.01	2086
	pCO_2, TA	4.99	4.10	2045
ΔpH	TA, TCO_2	0.0045	0.0087	2658
	TCO_2, pCO_2	-0.0076	0.0087	2086
	pCO_2, TA	-0.0065	0.0085	1948
ΔpCO_2	TA, pH	-15.7	19.2	1948
	pH, TCO_2	-16.3	18.5	2085
	TCO_2, TA	-22.0	19.7	2045

A16 South				
Parameter	**Input**	**Mean**	**Stdev**	**Number**
ΔTA	pH, TCO_2	-1.55	4.82	2361
	TCO_2, pCO_2	-5.74	4.34	718
	pCO_2, pH	57.83	32.78	673
ΔTCO_2	TA, pH	1.41	4.53	2361
	pH, pCO_2	57.35	29.52	700
	pCO_2, TA	5.03	3.71	718
ΔpH	TA, TCO_2	0.0023	0.0099	2361
	TCO_2, pCO_2	-0.0109	0.0056	700
	pCO_2, TA	-0.0099	0.0056	673
ΔpCO_2	TA, pH	-24.9	16.1	673
	pH, TCO_2	-25.1	15.3	700
	TCO_2, TA	-24.9	20.4	718

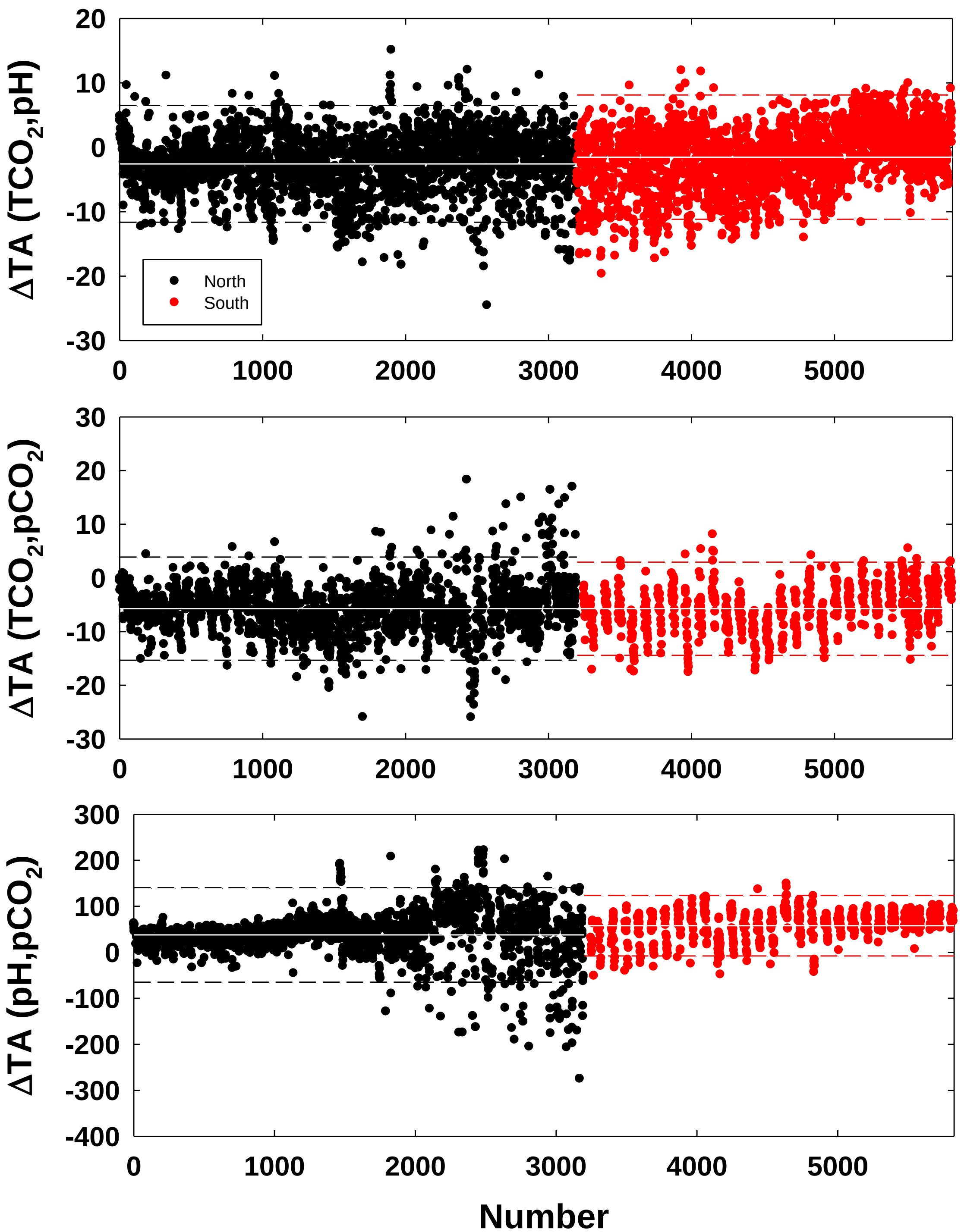

Figure 10. Difference between the measured and the calculated TA values. Inputs shown in parentheses. The dotted lines are the 2 standard deviation boundaries from the means (white lines).

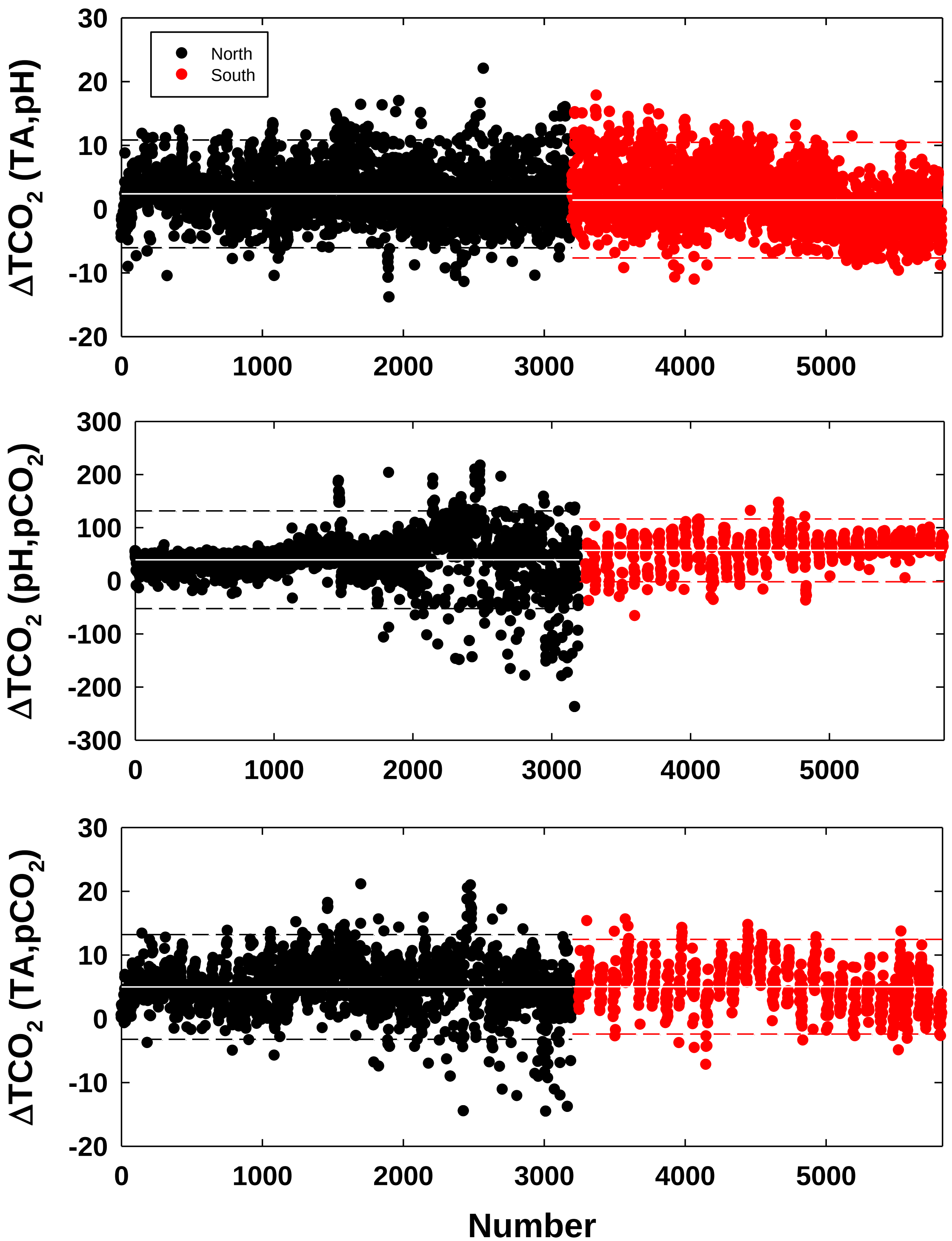

Figure 11. Difference between the measured and the calculated TCO_2 values. Inputs shown in parentheses. The dotted lines are the 2 standard deviation boundaries from the means (white lines).

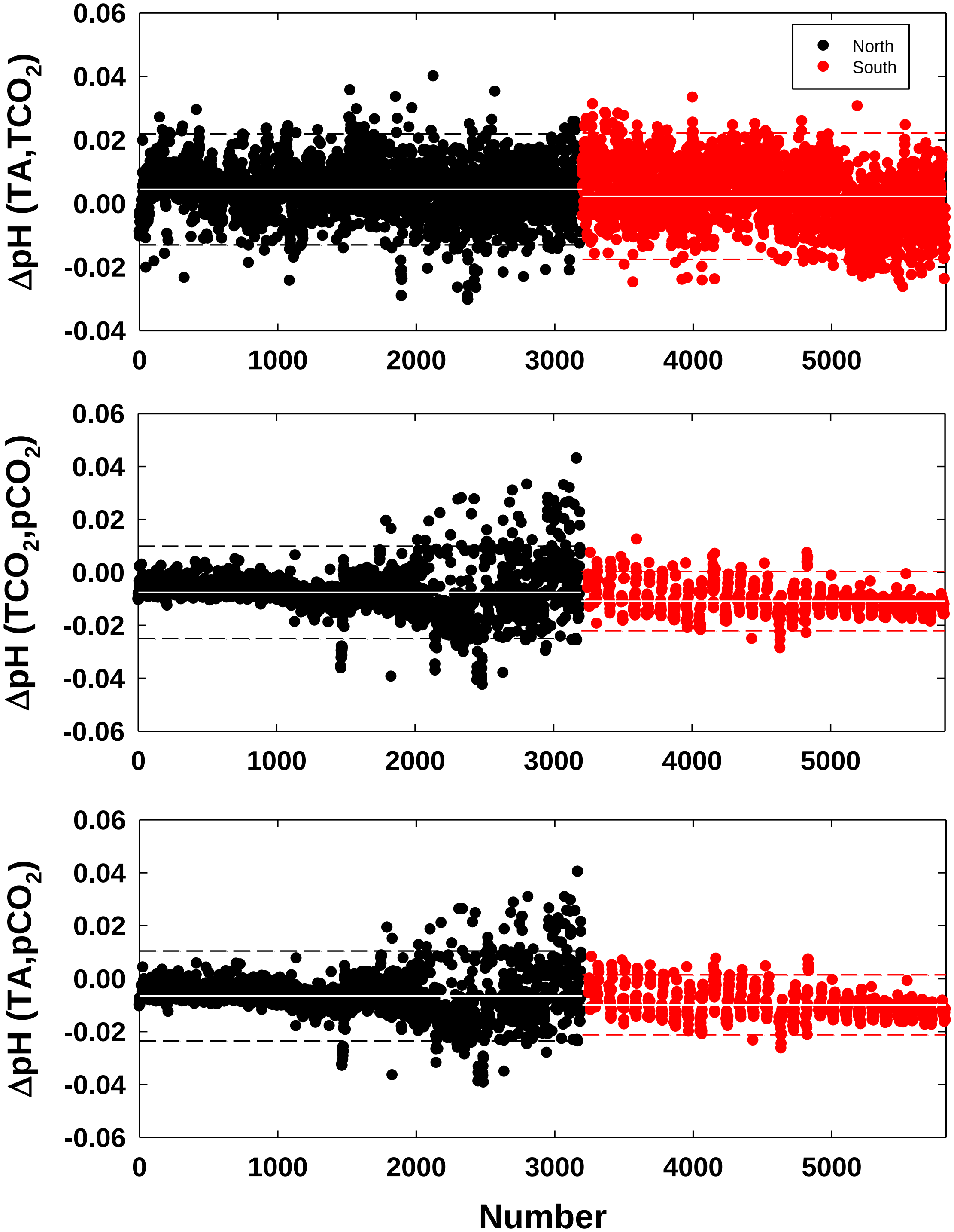

Figure 12. Difference between the measured and the calculated pH values. Inputs shown in parentheses. The dotted lines are the 2 standard deviation boundaries from the means (white lines).

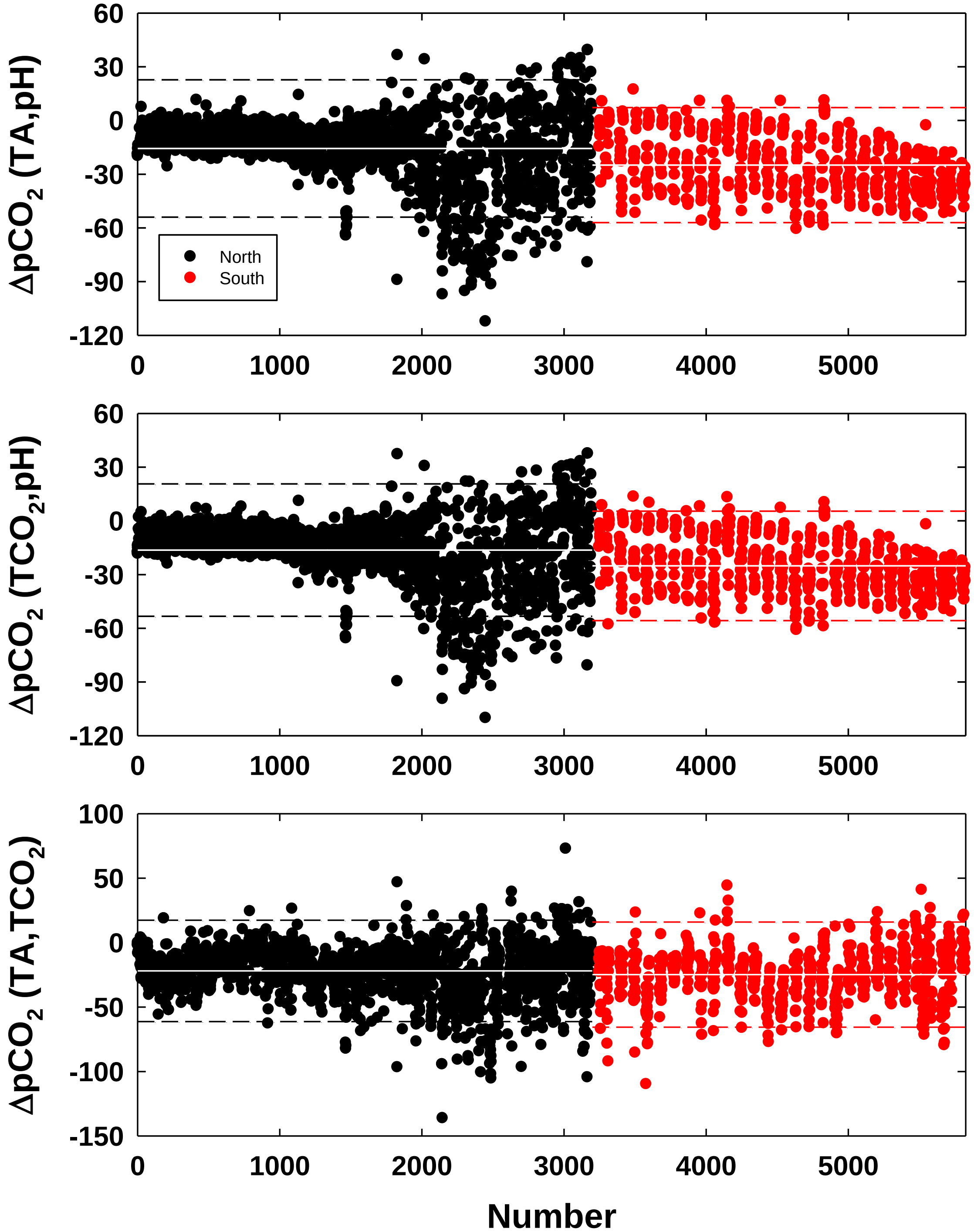

Figure 13. Difference between the measured and the calculated pCO_2 values. Inputs shown in parentheses. The dotted lines are the 2 standard deviation boundaries from the means (white lines).

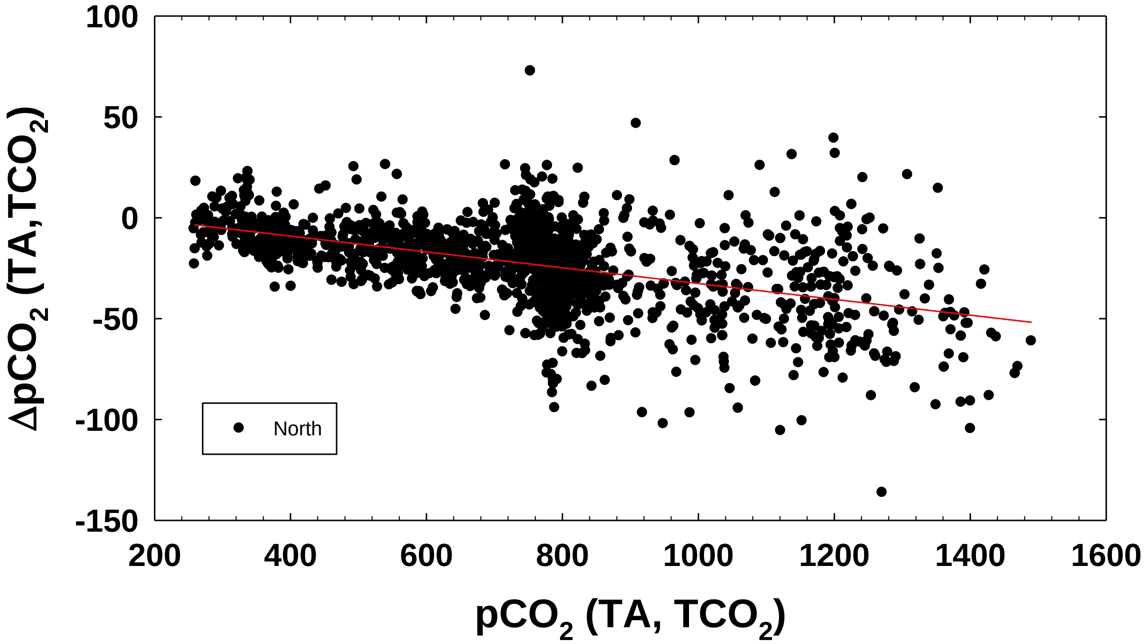

Figure 14. Difference between the measured and the calculated pCO_2 values as the calculated value of pCO_2 increases. Inputs shown in parentheses.

5. Distribution of the carbon parameters in seawater along the GO-SHIP A16N&S Track.

The section profile of TA is shown in **Figure 15,** that of TCO_2 measured by SOMMA is shown in **Figures 16**, and the spec. pH is shown on the seawater scale at 25º C in **Figure 17**. All sections were made using Ocean Data View (Schlitzer, 2012). Each figure is separated into two panels. The top panel shows the top 1000 db and the bottom panel shows from 1000 db to the seafloor. The North Atlantic Deep Water (NADW), Antarctic Intermediate Water (AAIW), and Antarctic Bottom Water (AABW) can clearly been seen in the sections.

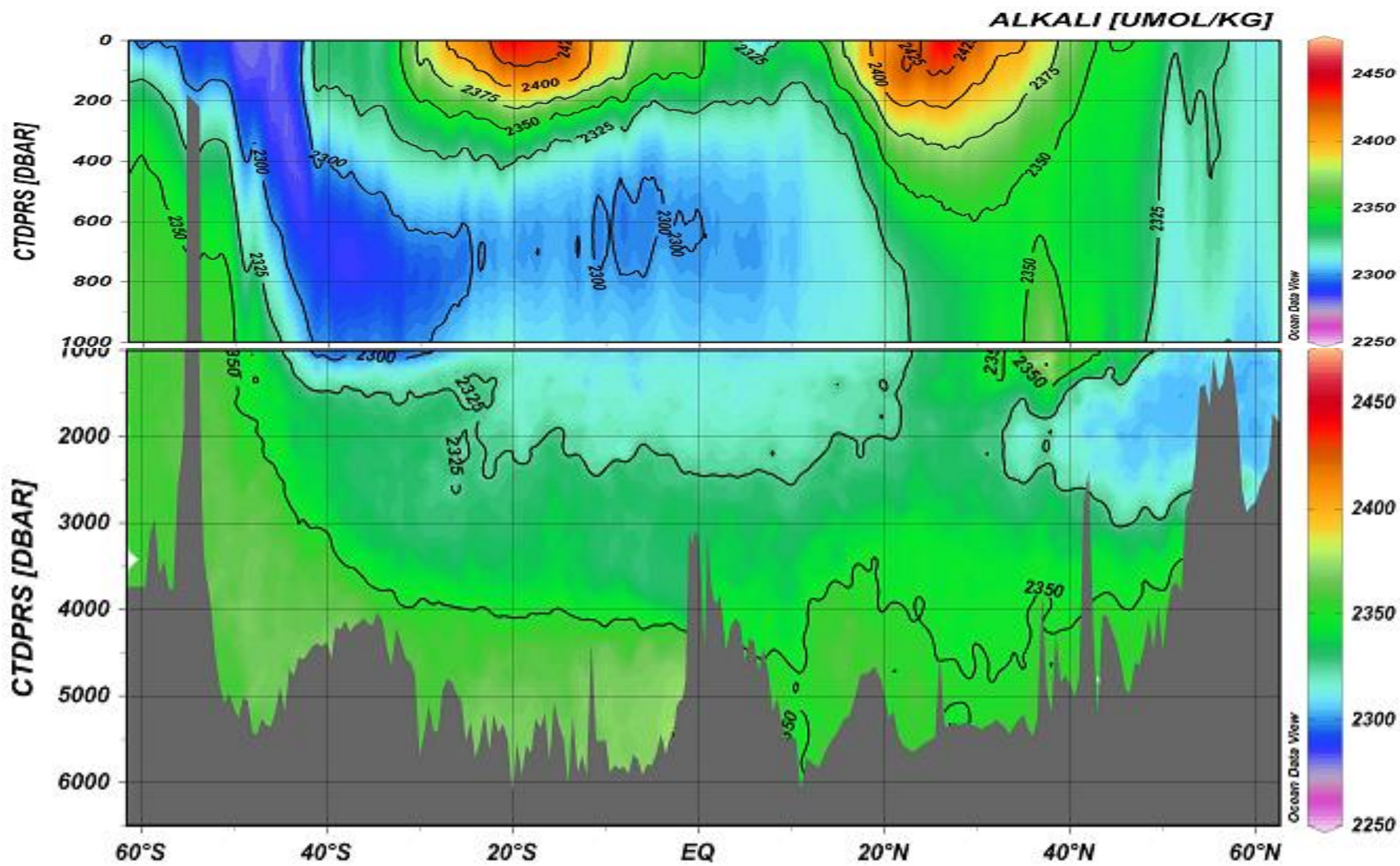

Figure 15. Measured total alkalinity in $\mu mol \cdot kg^{-1}$.

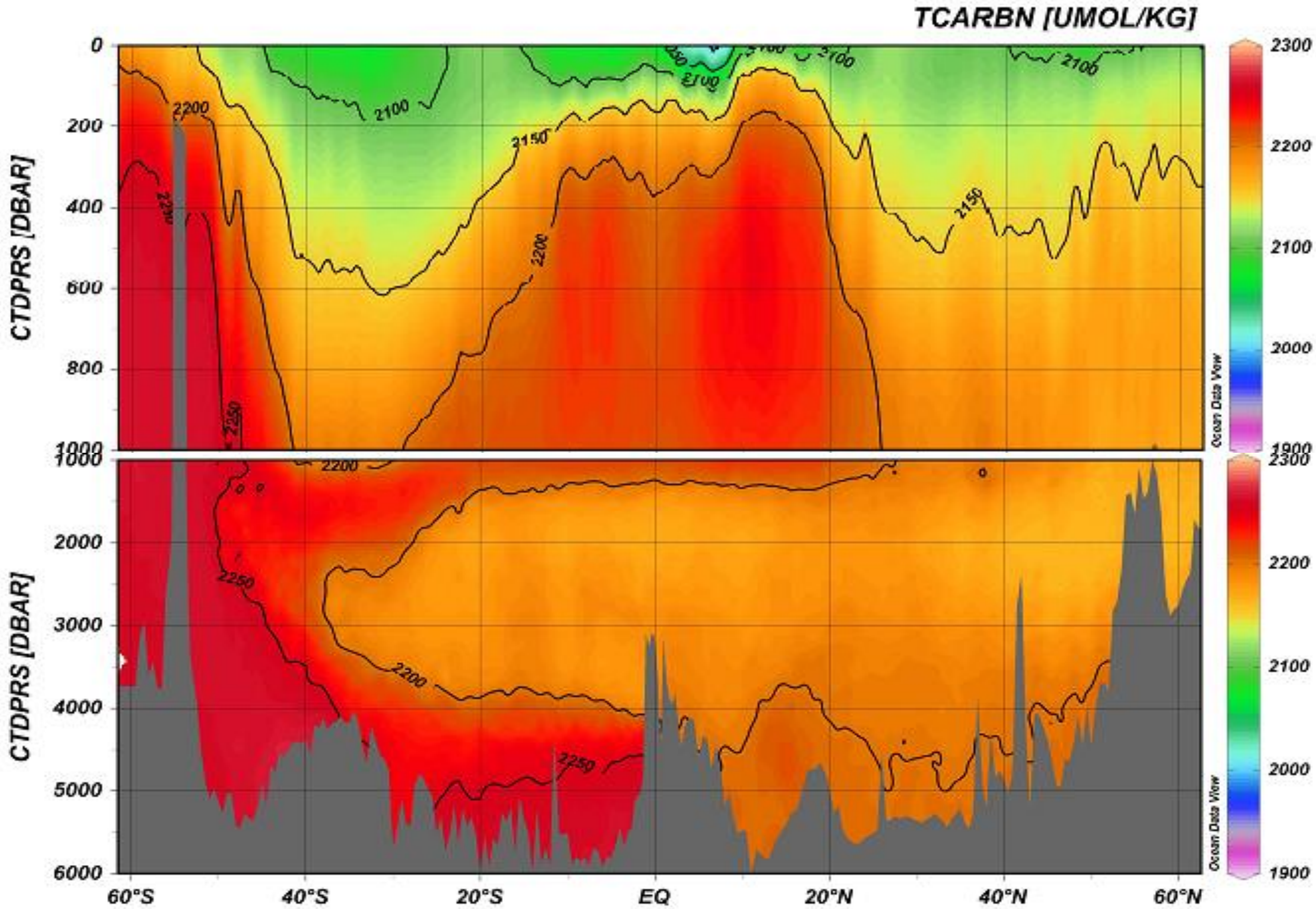

Figure 16. Measured TCO_2 (SOMMA) by coulometry in $\mu mol \cdot kg^{-1}$.

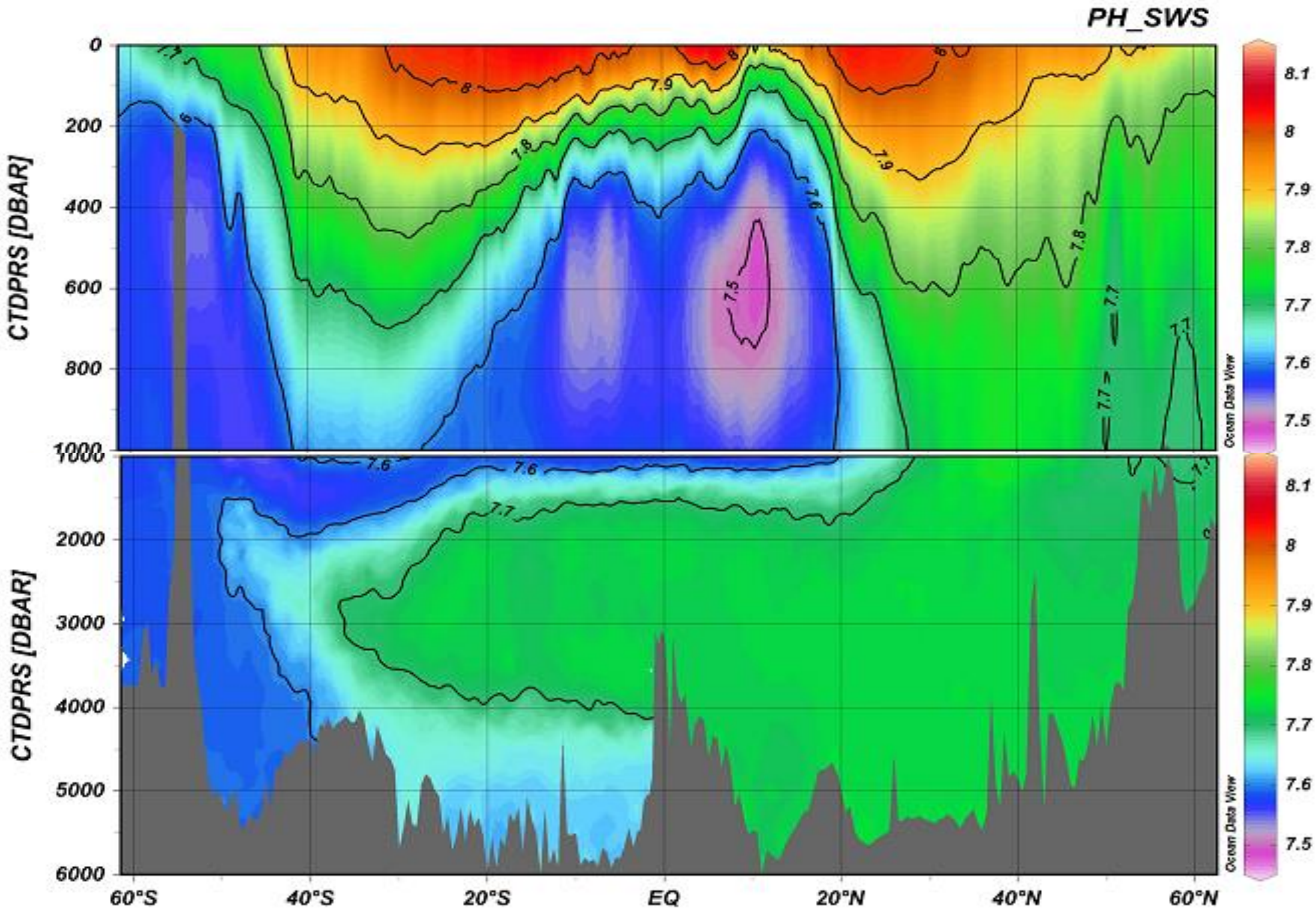

Figure 17. Measured spectrophotometric pH on the seawater scale at 25°C.

6. Crossover Points along A16 Cruise Track

Several crossover points occur along the cruise track. Since the line was broken into three separate legs, the final station of the previous leg was always reoccupied as the first station of the following leg. This results in a crossover point between A16N leg 1 and leg 2, and between A16N and A16S. There is also a crossover point at 30°S with the A10 cruise which was occupied in 2011. Profiles of the carbon parameters at the crossover points are shown in **Figures 18-20**. For the A16 North crossover between legs 1 and 2, the mean differences and standard deviations are -0.18 ± 6.62 for TA, 3.42 ± 6.85 for TCO_2, and -0.0058 ± 0.0115 for pH. For the crossover between the A16 North and the A16 South, the mean differences and standard deviations are -0.64 ± 7.34 for TA, 6.21 ± 13.63 for TCO_2, and -0.0141 ± 0.0324 for pH. For the A16/A10 crossover the mean differences and standard deviations for depths greater than 1000m are -1.48 ± 3.21 for TA, 1.55 ± 6.21 for TCO_2, and -0.0244 ± 0.0126 for pH. It's important to note that pH on A10 was potentiometric which has a lower precision than spec pH. The surface measurements are not included in the A16/A10 crossover because of seasonal and inter-annual variability, but the values are shown in the figures.

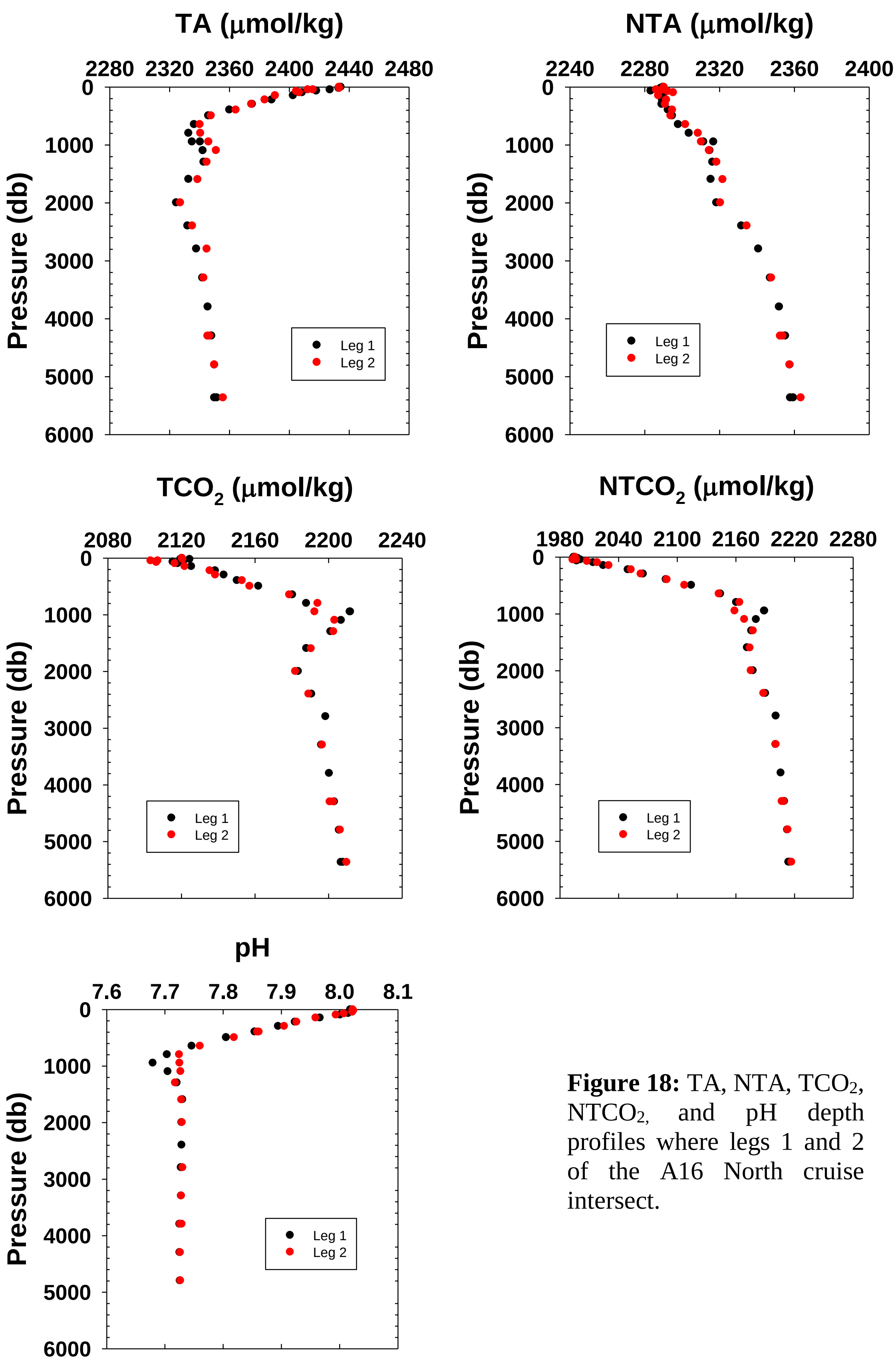

Figure 18: TA, NTA, TCO_2, $NTCO_2$, and pH depth profiles where legs 1 and 2 of the A16 North cruise intersect.

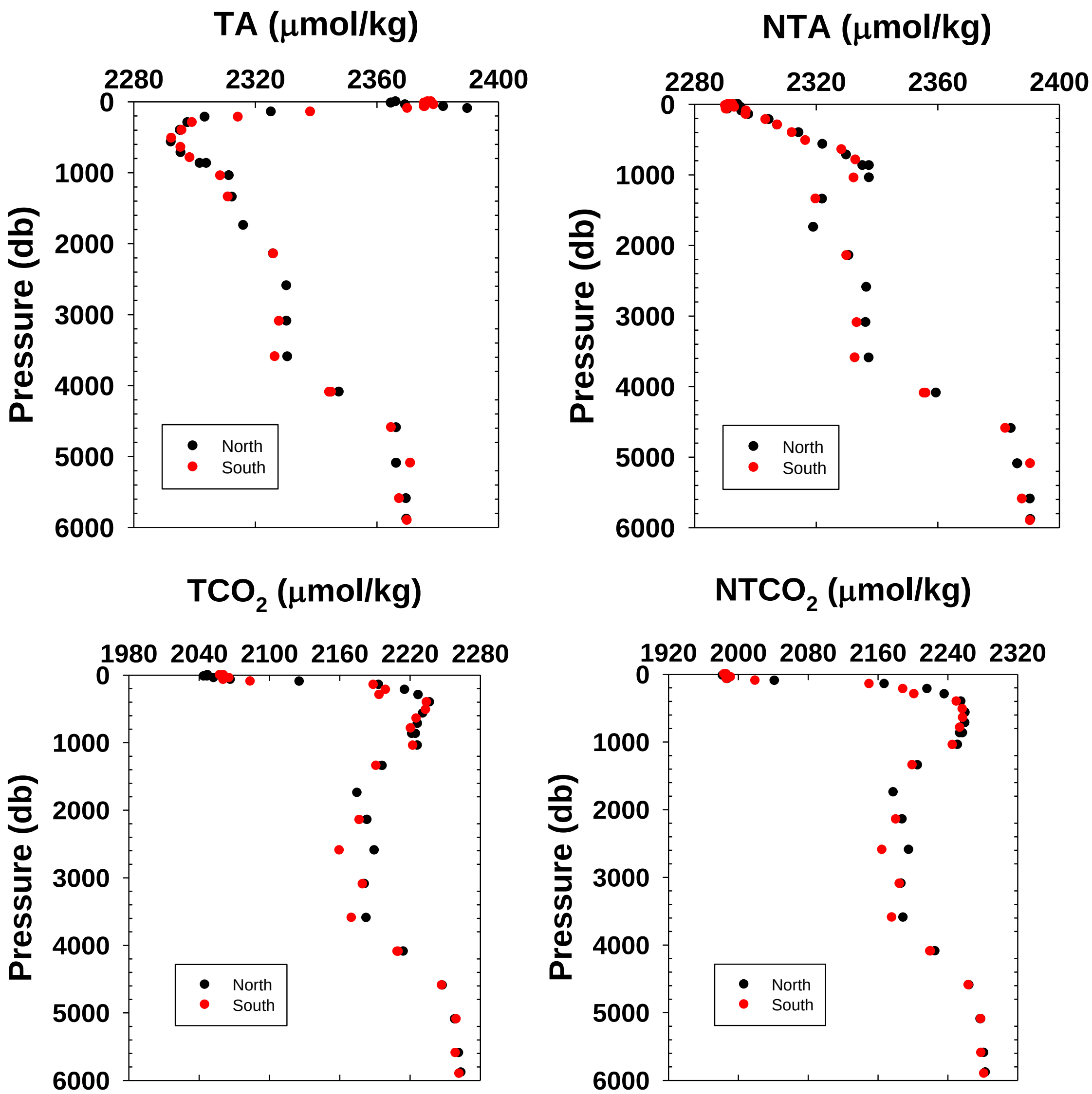

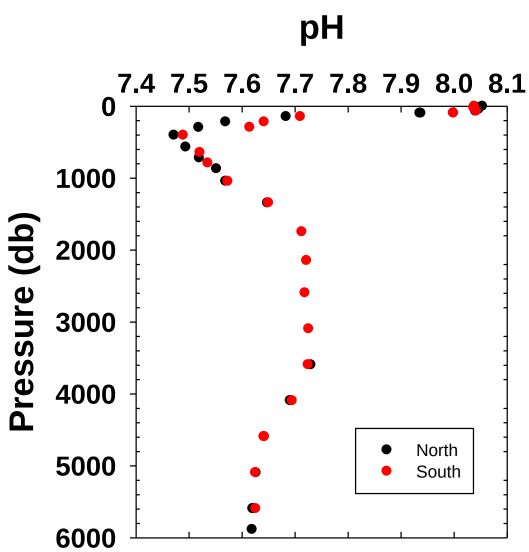

Figure 19: TA, NTA, TCO_2, $NTCO_2$, and pH depth profiles where the A16 North and A16 South cruises intersect.

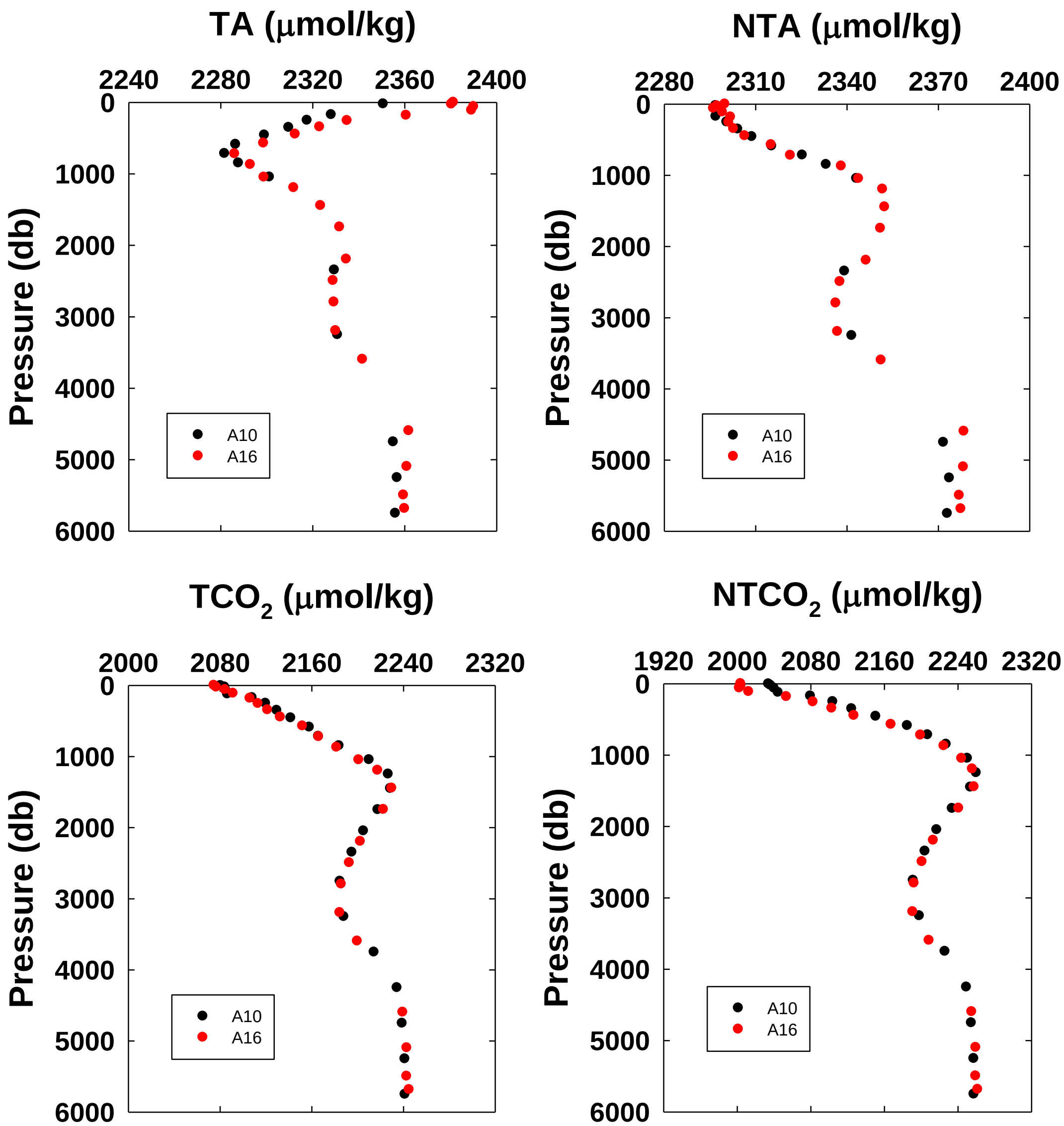

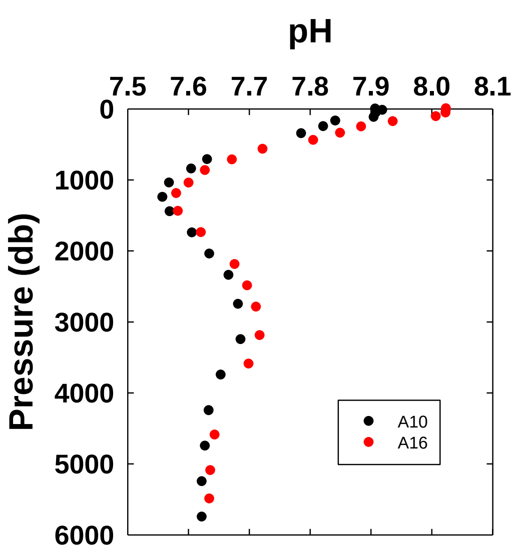

Figure 20: TA, NTA, TCO_2, $NTCO_2$, and pH depth profiles at 25.0°W and 30.0°S where the A10 cruise and the A16 cruise intersect.

7. Surface Measurements of the 1988/89, 1991/93, 2003/5, and 2013/14 Cruises

The A16 line has now been occupied 4 times over the last 26 years. The first time was in 1988/89 as part of the South Atlantic Ventilation Experiment (SAVE), it was then repeated a few years later in 1991/93 as part of the Ocean Atmosphere Carbon Exchange Study (OACES), In 2003/5 it was occupied as part of the CLIVAR program, and the most recent occupation in 2013/14 as part of GO-SHIPS. These acronyms will be used to identify the separate occupations of the cruise track. The locations of the stations may not be exact repeats, most are within 0.5 nm. We defined the surface measurements by determining the depth of the mixed layer using temperature and salinity profiles. These surface measurements from all four occupations of salinity and oxygen are illustrated in **Figure 21**, that of TA, TCO_2 and pH in **Figure 22**, and that of NTA and $NTCO_2$ in in **Figure 23**. An increase in TCO_2 as a result of uptake of anthropogenic CO_2 is clearly visible; there is also a clear decrease in the surface pH. The pH values for the OACES cruises show a lot of scatter, the 1991 cruise was potentiometric pH which is less precise than spec. pH, and the 1993 cruise was one of the first times that the spec. pH method was used.

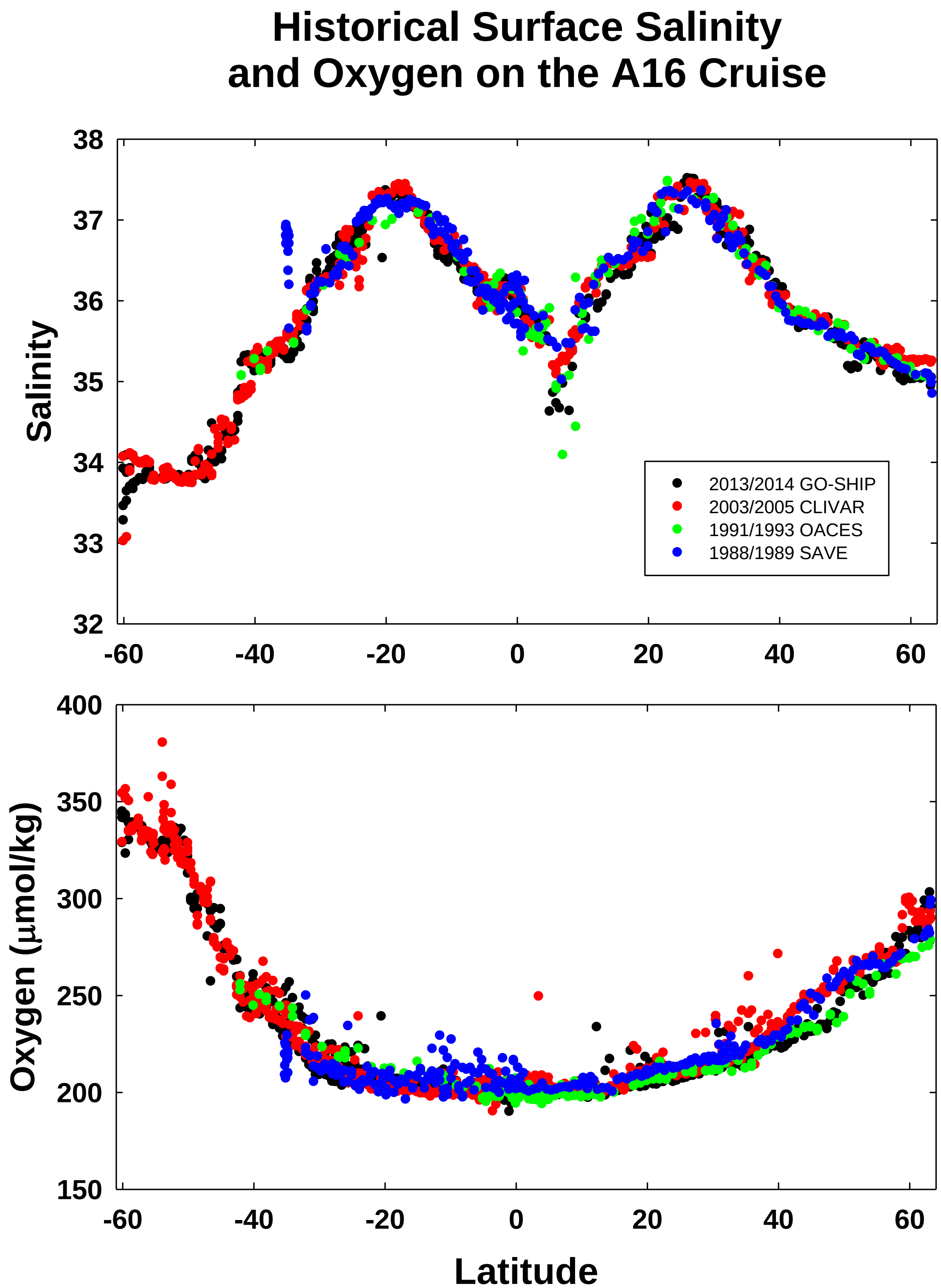

Figure 21. Surface salinity and oxygen values measured during the A16 cruises from 1988 to 2014.

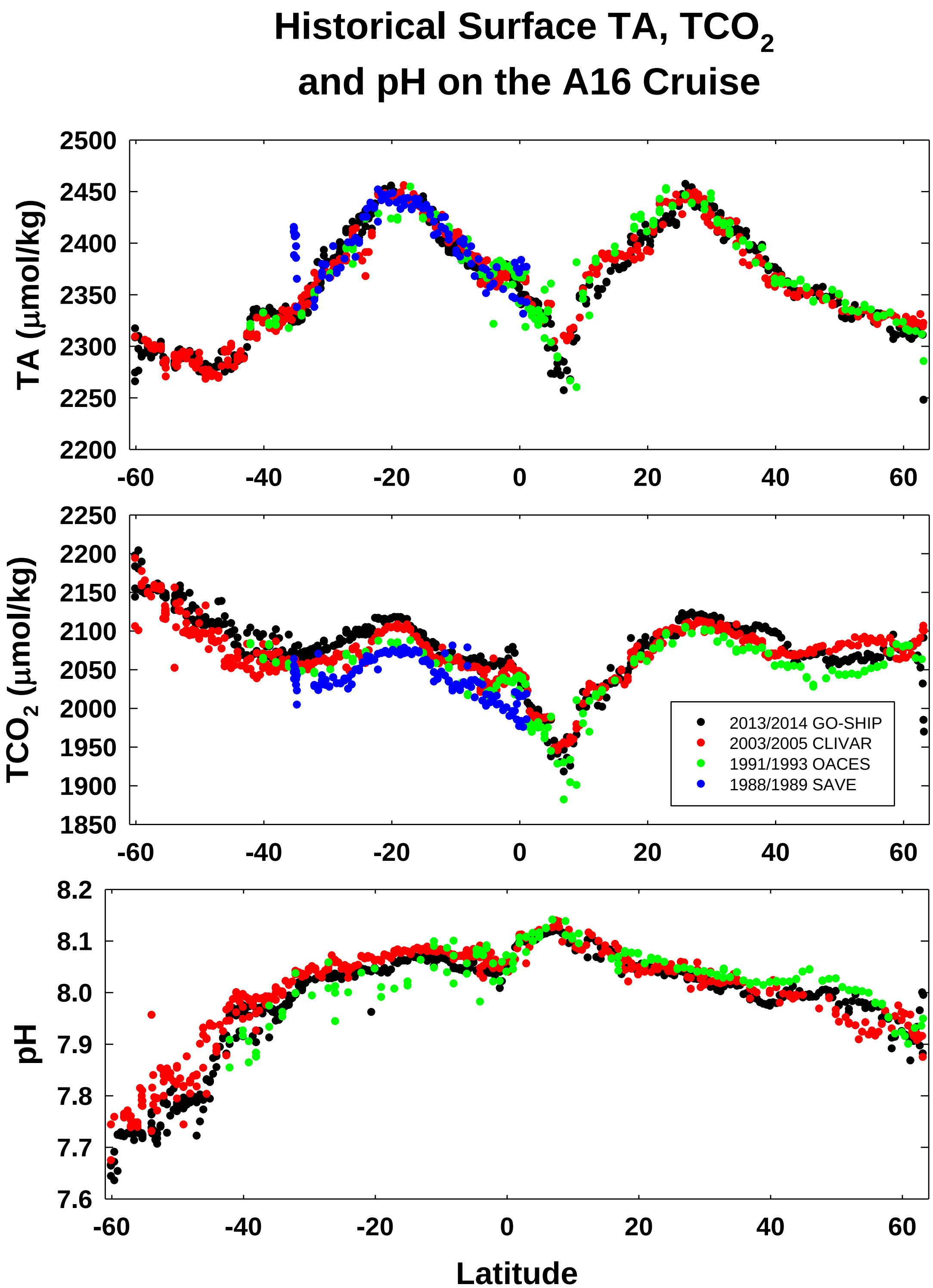

Figure 22. Surface TA, TCO_2 and pH values measured during the A16 cruises from 1988 to 2014.

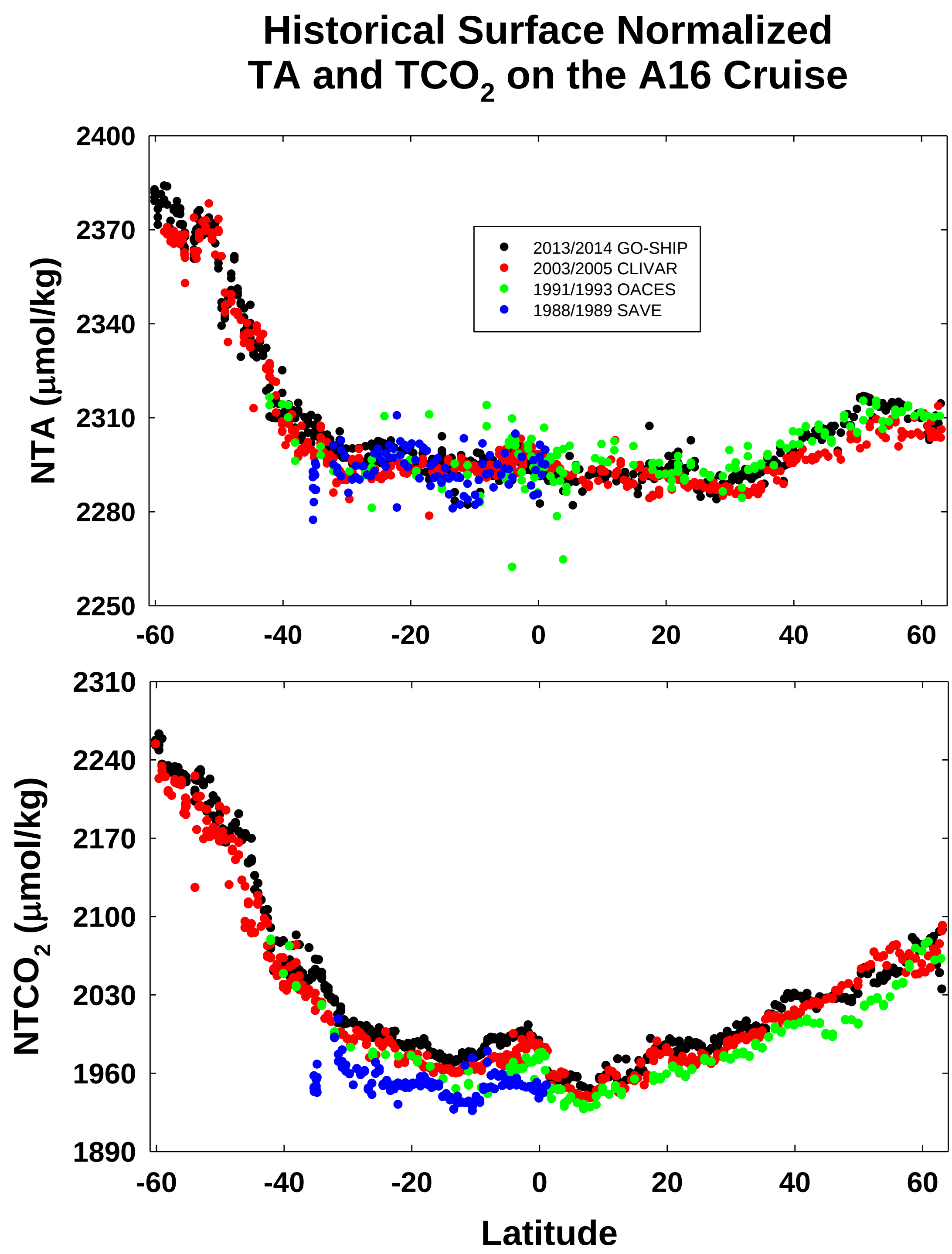

Figure 23. Surface NTA and $NTCO_2$ values measured during the A16 cruises from 1988 to 2014.

8. Decadal Changes of the Carbon Parameters

Comparison of the total alkalinity, total inorganic carbon dioxide, and pH measurements collected in the A16 cruises from GO-SHIP, CLIVAR, OACES, and SAVE cruises are illustrated in **Figures 24-31**. The greatest changes in TCO_2 and pH occur at depths above 1000 meters, as would be expected due to variation in biological productivity and anthropogenic input of CO_2, while generally TA remains nearly constant within ± 5 $\mu mol \cdot kg^{-1}$ across the column and longitude of the cruise, larger variations do occur when comparing the older cruises. All three carbon parameters were measured on the OACES, CLIVAR, and GO-SHIP cruises. The pH on the southern portion of the OACES cruise was measured by potentiometer, while the pH on the northern portion of OACES and all of the CLIVAR and GO-SHIP cruises was measured by spectrophotometer. No carbon parameters were measured on the WOCE 1988 cruise and only TA and TCO_2 were measured on the 1989 WOCE (SAVE) cruise.

8.1 Changes between the CLIVAR 2003/5 and the GO-SHIP 2013/14

Figure 24 shows that normalized total alkalinity is generally constant between the CLIVAR and GO-SHIP occupations within about ±5 $\mu mol \cdot kg^{-1}$. This is approximately the accuracy of the measurements and is as expected since uptake of anthropogenic CO_2 doesn't affect the alkalinity. The southern portion shows more variability (~10 $\mu mol \cdot kg^{-1}$) than the northern portion. **Figure 25** shows that deep values of $NTCO_2$ are generally constant within the accuracy of the measurements, but that surface values show large increases as would be expected from the uptake of CO_2. Some areas show decreases in $NTCO_2$ which correspond to changes in oxygen as well, indicating differences in biological activity. **Figure 26** shows that deep pH values were constant within the uncertainty of the measurements, and decreased in the surface ocean as expected from uptake of anthropogenic CO_2, with a rather large increase near the equator, which also corresponds to decreases in TCO_2. This might indicate changes in productivity or water circulation.

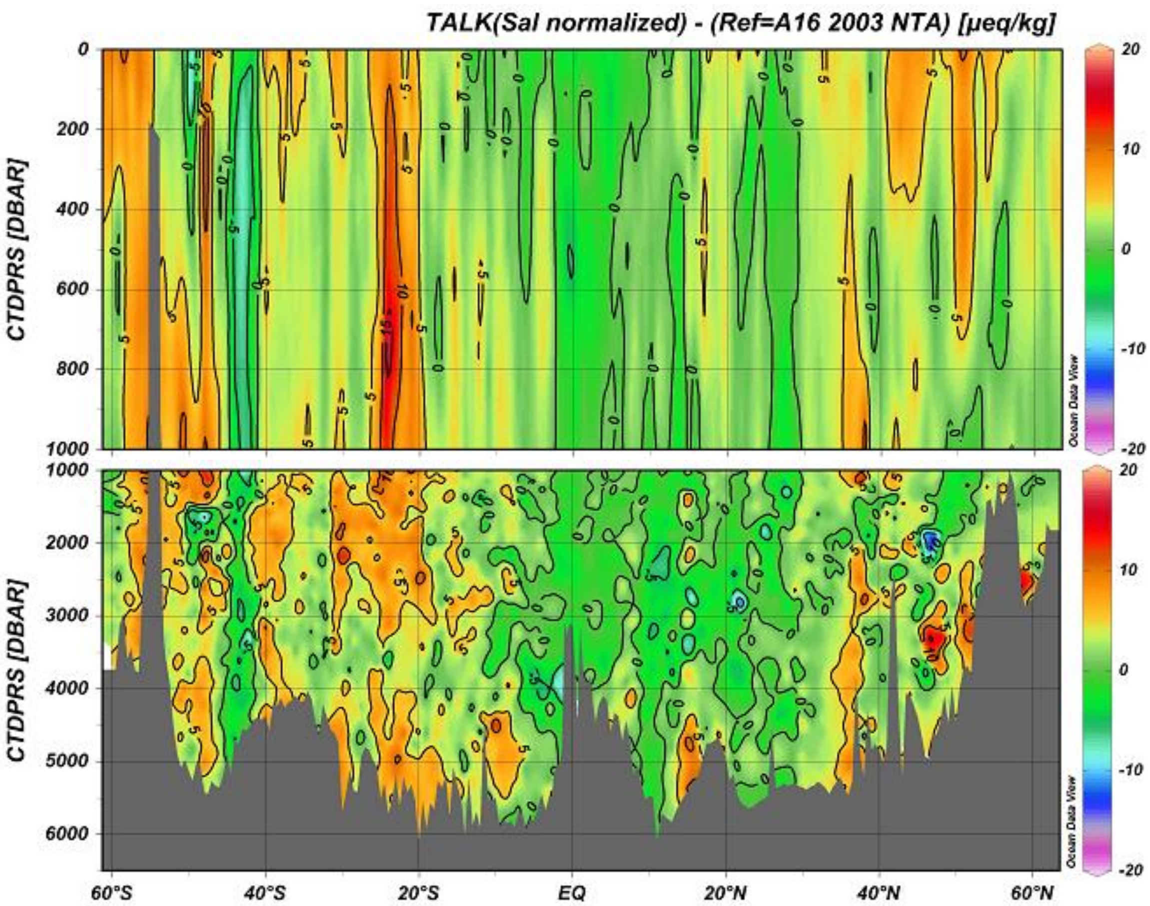

Figure 24. Changes in NTA (μmol·kg^{-1}) between the CLIVAR (2003/5) and GO-SHIP (2013/14) cruises.

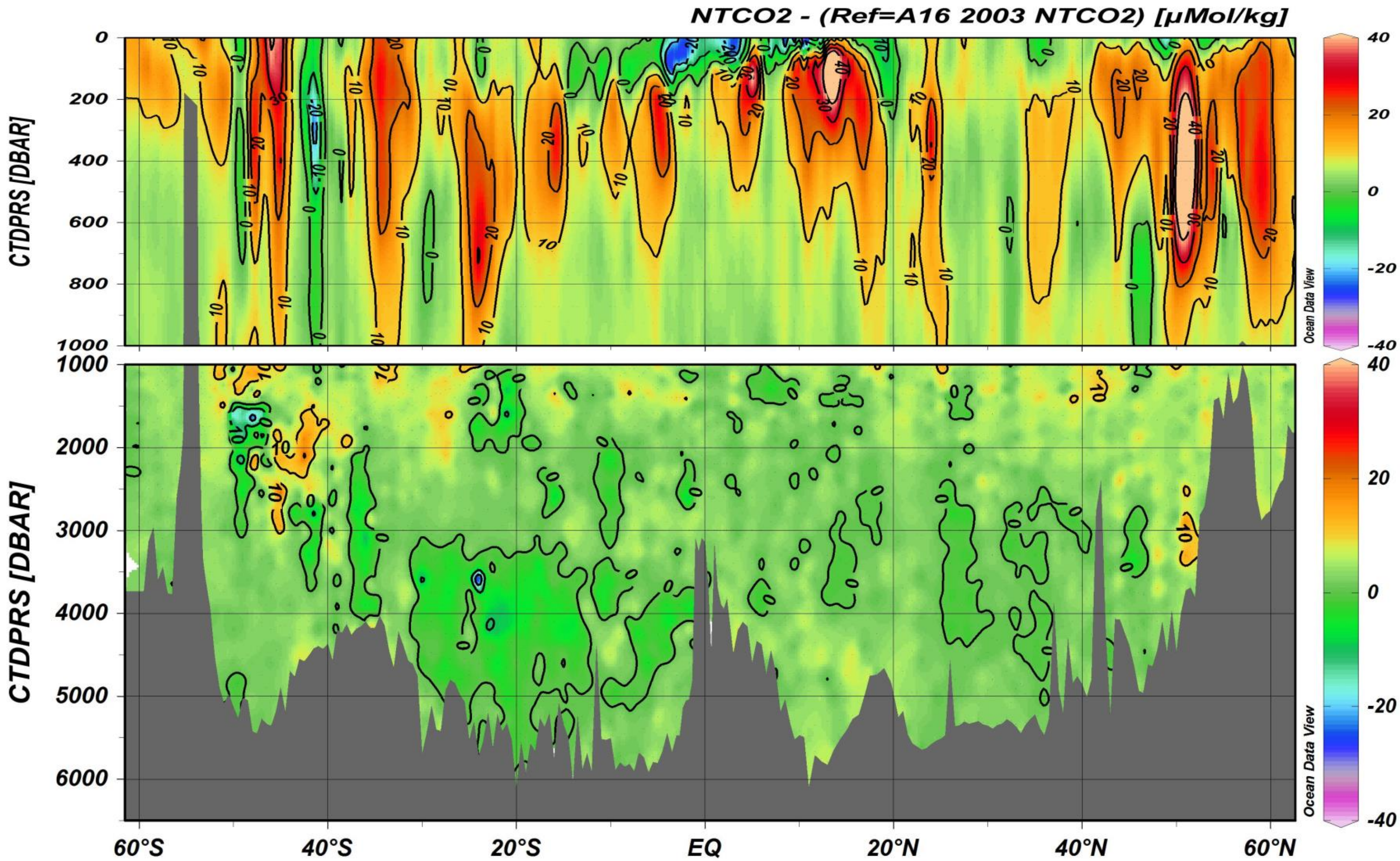

Figure 25. Changes in $NTCO_2$ ($\mu mol \cdot kg^{-1}$) between the CLIVAR (2003/5) and GO-SHIP (2013/14) cruises.

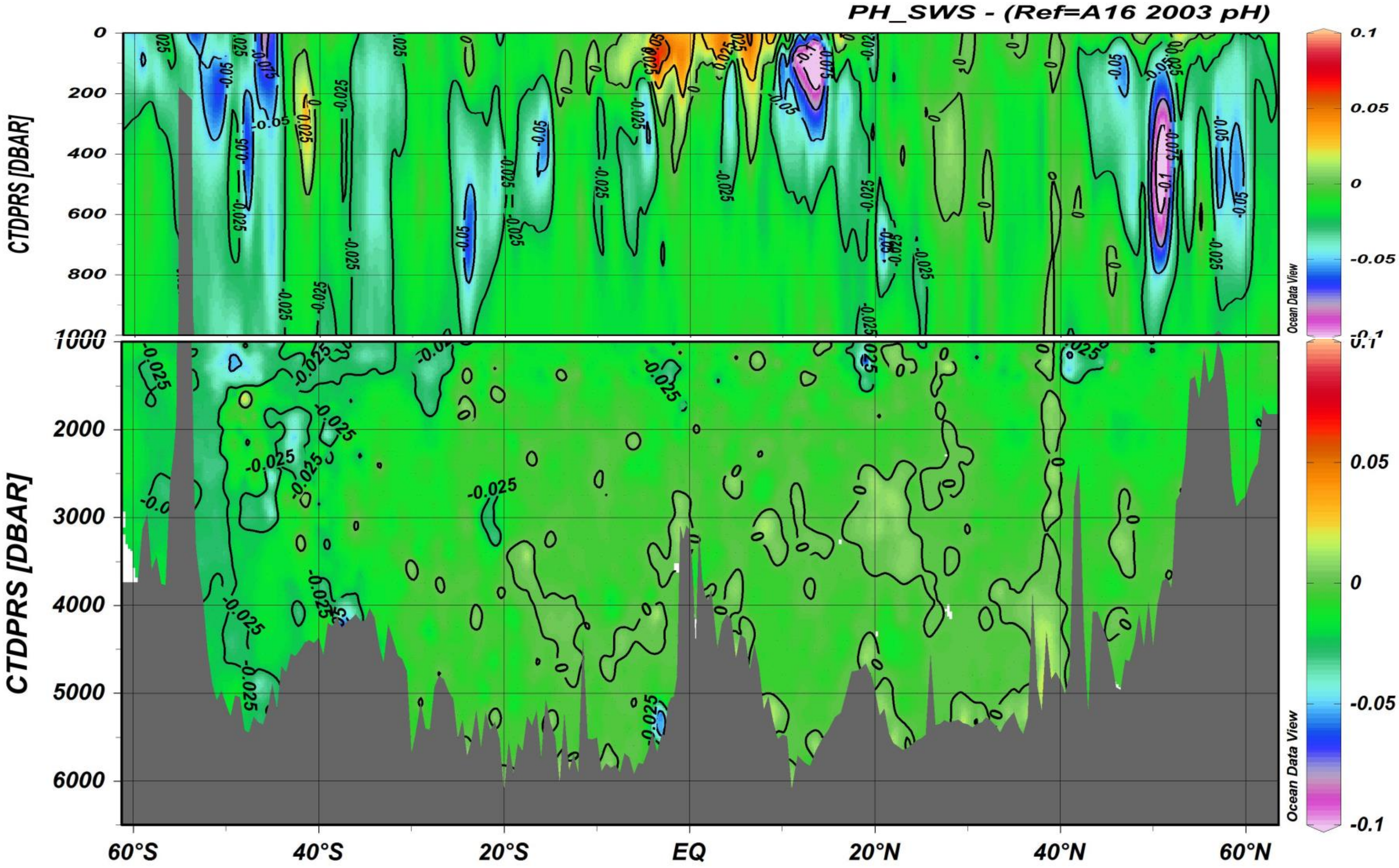

Figure 26. Changes in pH between the CLIVAR (2003/5) and GO-SHIP (2013/14) cruises.

8.2 Changes between the OACES 1991/93 and the GO-SHIP 2013/14

Figure 27 shows that NTA remained generally constant between the OACES and GO-SHIP cruises over the northern portion of the cruise track and are generally within the uncertainty of the measurements. There is a larger variability than expected in the southern portion of the cruise. During the OACES 1991 cruise a computer failed and the titrations were run by hand, these profiles show a larger amount of scatter indicating a lower precision in the measurements. The sampling pattern on the OACES cruises was also of lower resolution than the GO-SHIP cruise so some of the changes may be an artifact of interpoltion of the data. **Figure 28** shows a similar pattern for the changes in the $NTCO_2$ between the two cruises as that shown in **Figure 25** with changes in deep water for the northern portion being near the precision of the measurements but some portions of the southern cruise having decreases of around 10 $\mu mol \cdot kg^{-1}$. There's a larger increase in surface waters than found between the CLIVAR/GO-SHIP; as expected from the input of anthropogenic carbon over the longer time period. **Figure 29** shows the changes in pH. Only the northern portion is shown because the southern cruise used potentiometric pH and the profiles showed too much scatter to reliably determine decadal changes. Calculating pH from TA and TCO_2 would provide more reliable results. As expected there is a general decrease in pH in surface waters due to the uptake of anthropogenic CO_2. The magnitude is roughly consistent with the expected decrease over a 20 year period. Changes in pH are detectable all the way to the bottom in the northern most portion of the cruise, elsewhere the deep waters show no detectable change.

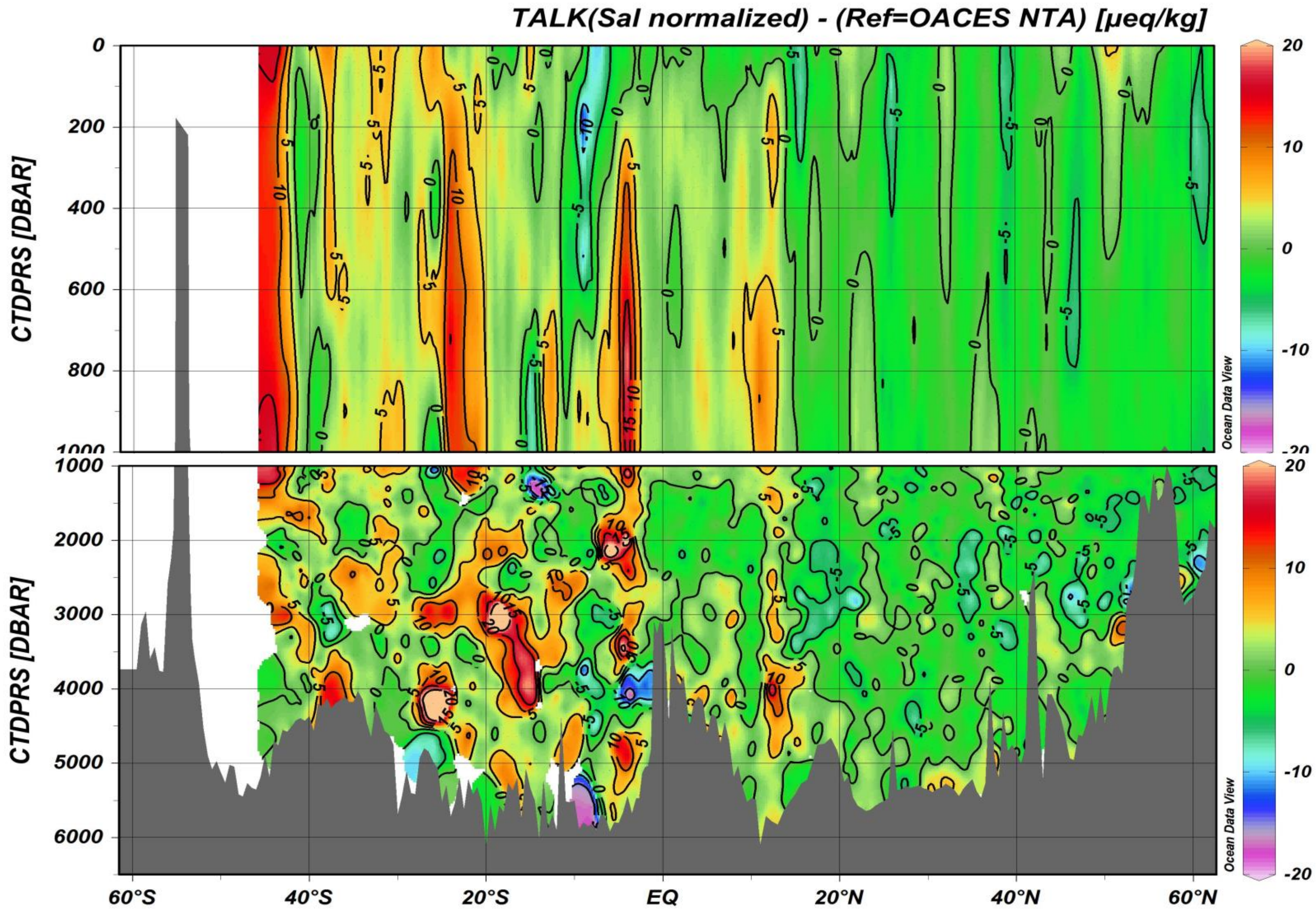

Figure 27. Changes in NTA ($\mu mol \cdot kg^{-1}$) between the OACES (1991/93) and GO-SHIP (2013/14) cruises.

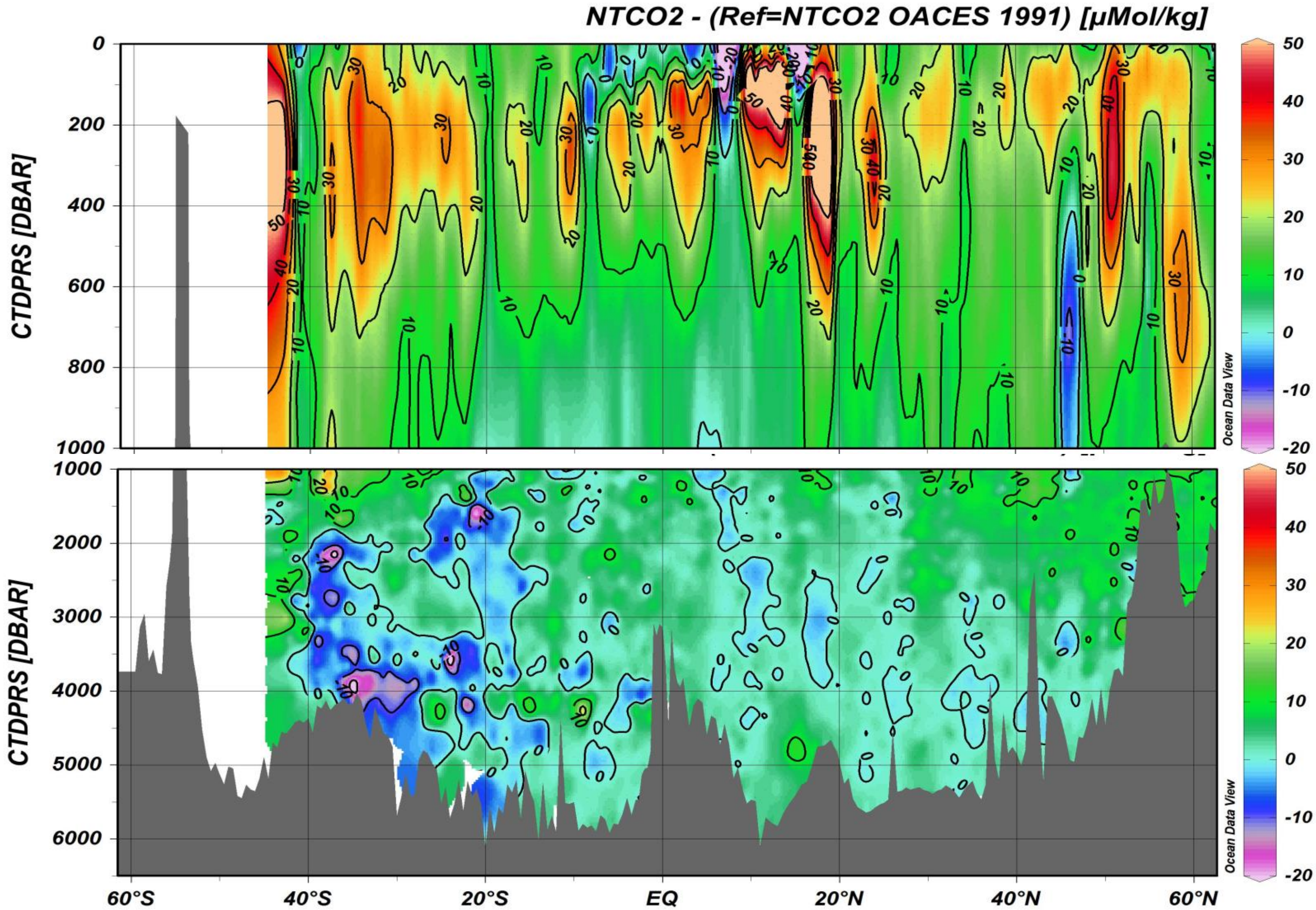

Figure 28. Changes in $NTCO_2$ ($\mu mol \cdot kg^{-1}$) between the OACES (1991/93) and GO-SHIP (2013/14) cruises

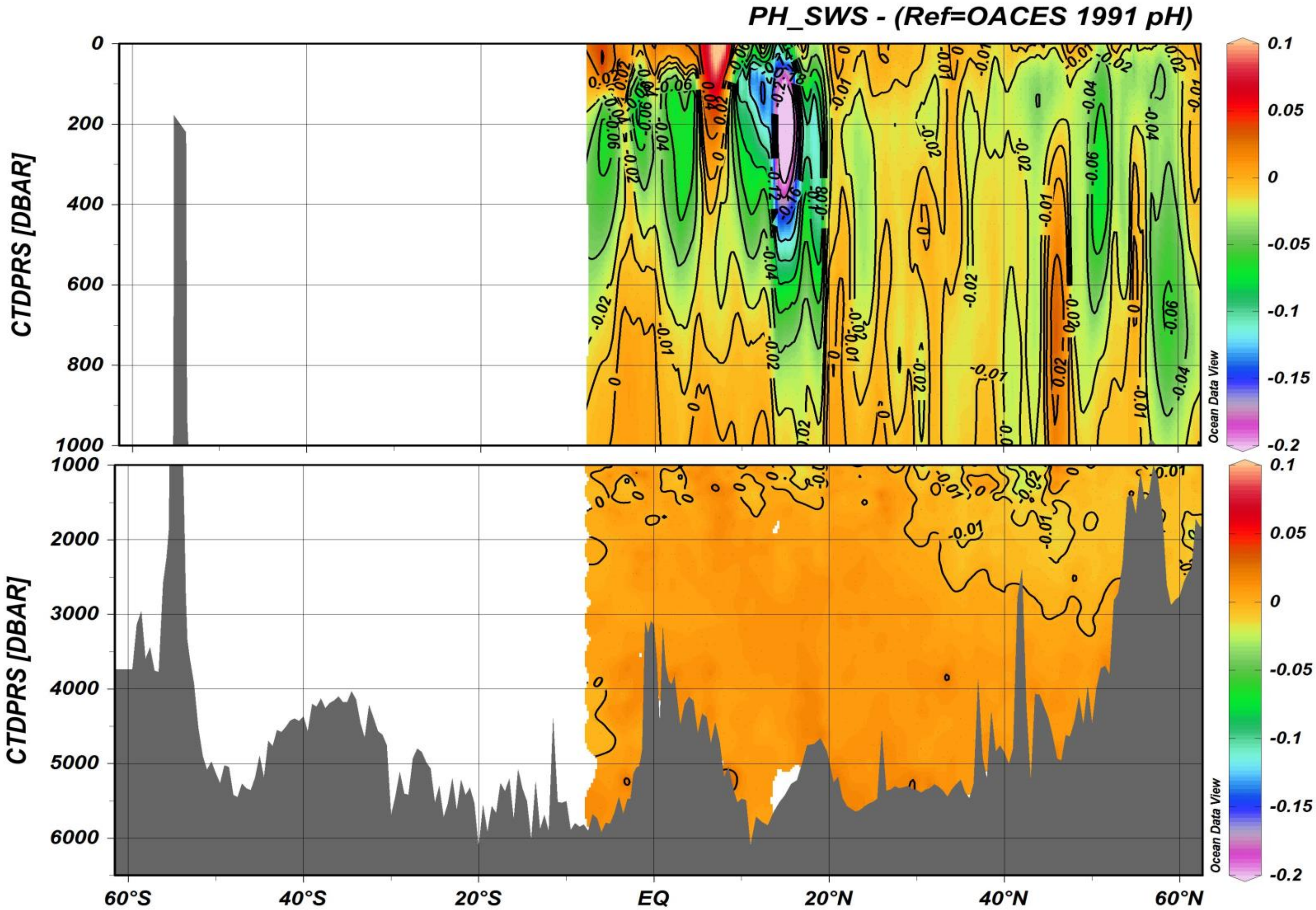

Figure 29. Changes in pH between the OACES (1993) and GO-SHIP (2013/14) cruises. The OACES 1991 cruise is not shown (see text).

8.3 Changes between the SAVE 1988/89 and the CLIVAR 2013/14

The A16 cruise track was first occupied in 1988 and 1989 as part of WOCE under the South Atlantic Ventilation Experiment (SAVE). Carbon parameters were not measured on the northern portion and only TA and TCO_2 were measured on the southern portion. **Figure 30** shows the changes in normalized total alkalinity over the 25 years for the region where data is available. Although large portions show no change within the expected precision there are also some areas that show large increases or decreases. Certified reference material didn't become available until 1990 so the quality of these earlier measurements is probably lower then more recent ones. **Figure 31** shows the changes in normalized TCO_2. Large increases of 30-60 $\mu mol \cdot kg^{-1}$ occur in the surface as expected from anthropogenic carbon uptake; however there is larger than expected variability in the deep water with some areas being $\pm$ 15 $\mu mol \cdot kg^{-1}$. This could be a result of there being no CRMs for the 1989 cruise.

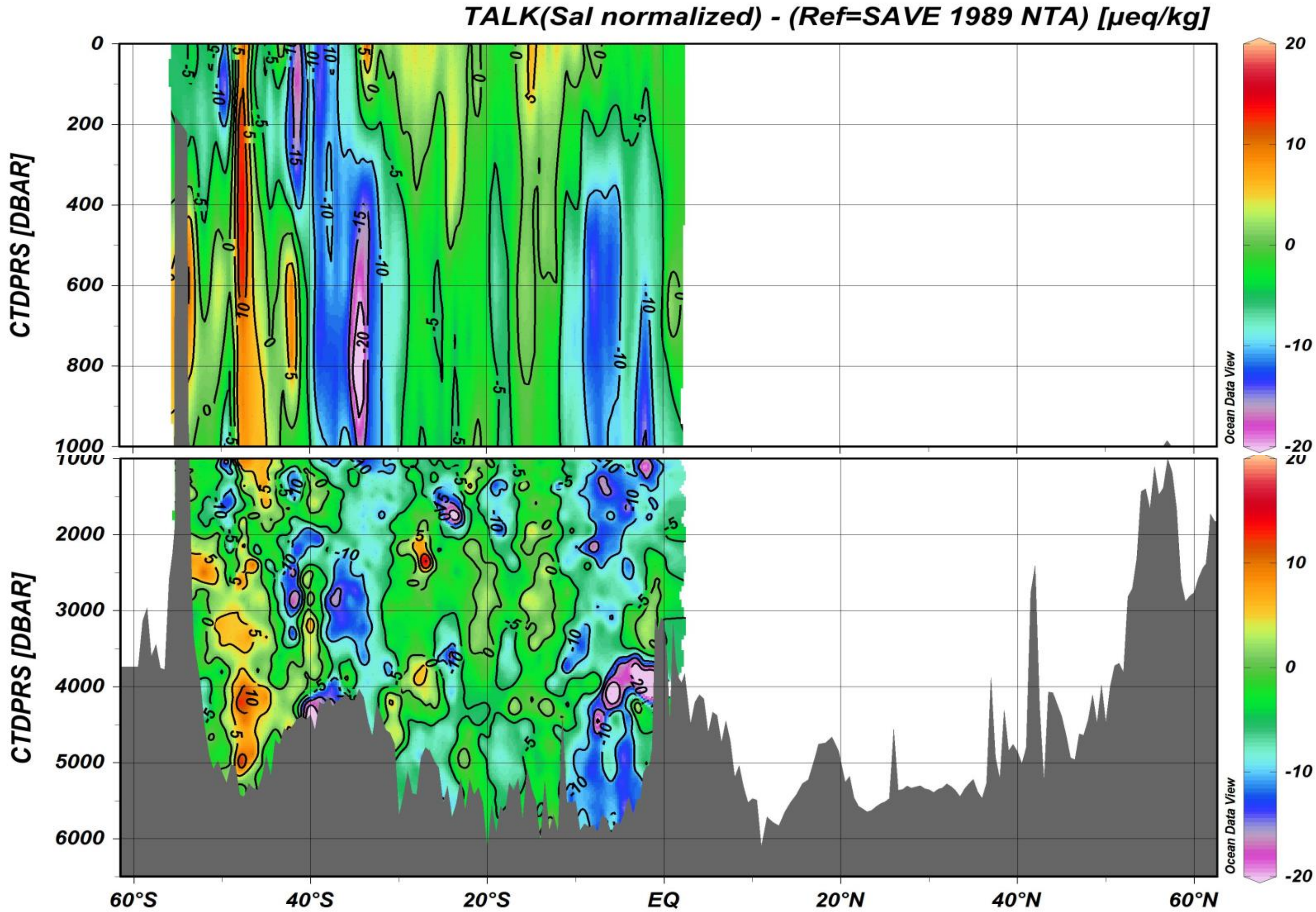

Figure 30. Changes in NTA (μmol·kg^{-1}) between the SAVE (1989) and GO-SHIP (2013/14) cruise.

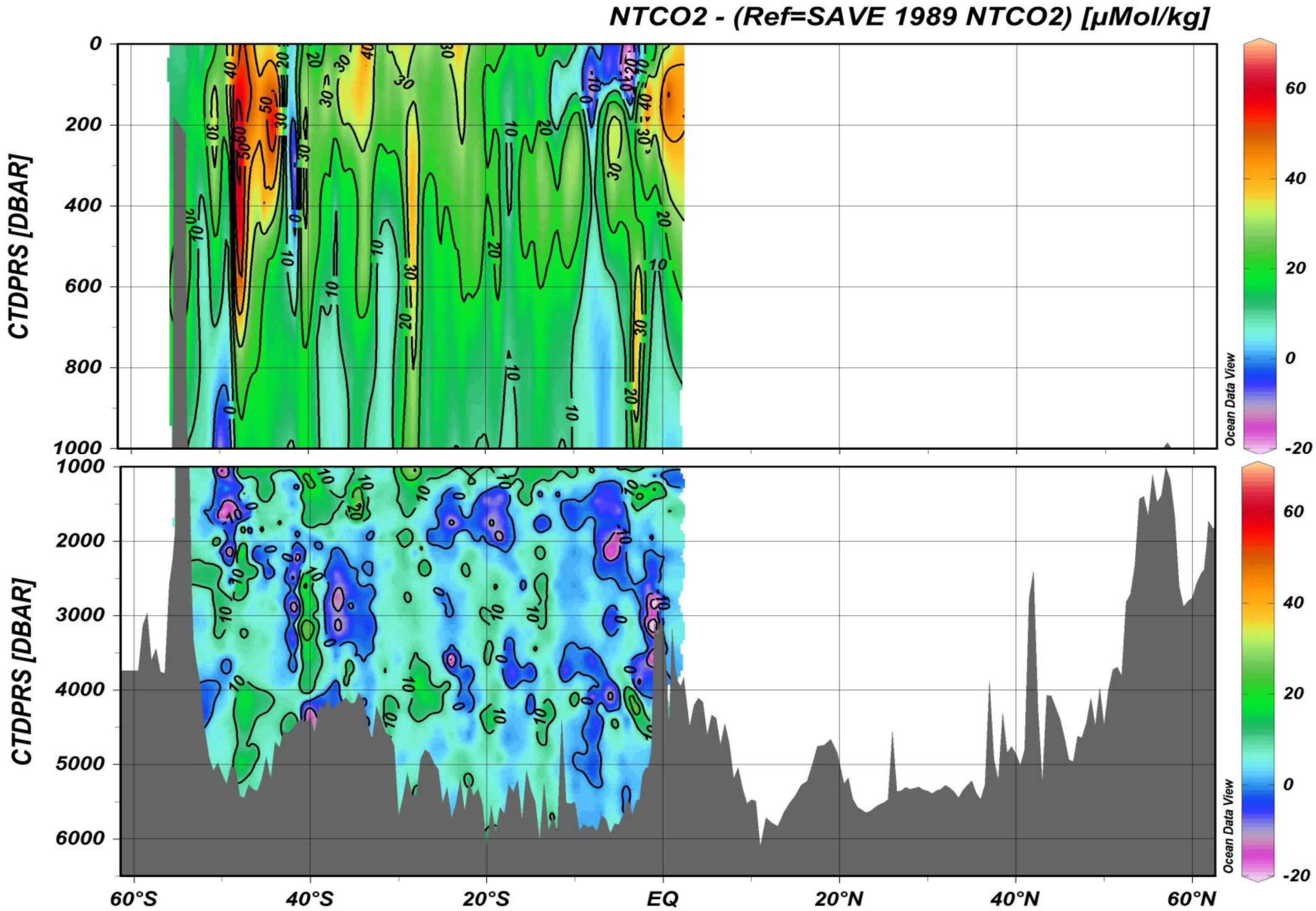

Figure 31. Changes in the NTCO₂ (μmol·kg⁻¹) between the SAVE (1989) and GO-SHIP (2013/14) cruises

References

Clayton, T.D., and R.H. Byrne, 1993: Spectrophotometric seawater pH measurements: Total hydrogen ion concentration scale calibration of m-cresol purple and at-sea results. *Deep-Sea Res.*, **40**, 2315-2329.

Dickson, A.G., 1990: Thermodynamics of the dissociation of boric acid in synthetic seawater from 273.15 to 318.15 K. *Deep-Sea Res., Part A,* **37**, 755-766.

Dickson, A.G., and J.P. Riley, 1979: The estimation of acid dissociation constants in seawater media from potentiometric titration with strong base, 1: The ionic product of water-KSUS-w. *Mar. Chem.*, **7**, 89-99.

Dickson, A.G., 1981: An exact definition of total alkalinity and a procedure for the estimation of alkalinity and total CO_2 from titration data. *Deep-Sea Res., Part A,* **28**, 609-623.

Dickson, A.G., Sabine, C.L. and Christian, J.R. (Eds.) 2007. Guide to best practices for ocean CO_2 measurements. PICES Special Publication 3, 191 pp.

Hoppe, C.J.M., Langer, G., Rokitta, S.D., Wolf-Gladrow, D.A. and Rost, B., 2012: Implications of observed inconsistencies in carbonate chemistry measurements for ocean acidification studies. *Biogeosciences*, **9**, 2401-2405.

Johansson, O., and M. Wedborg, 1982: On the evaluation of potentiometric titrations of seawater with hydrochloric acid. *Oceanologica Acta,* **5**, 209-218.

Lee, K., F.J. Millero and D.M. Campbell, 1996: The reliability of the thermodynamic constants for the dissociation carbonic acid in seawater, Mar. Chem., **55** 233-246.

Lee, K., T-W. Kim, R.H. Byrne, F.J. Millero, R.A. Feely, and Y-M. Liu, 2010: The universal ratio of boron to chlorinity for the North Pacific and North Atlantic oceans, Geochim. Cosmochim. Acta, **74**, 1801-1811.

Liu, X., M.C. Patsavas, and R.H. Byrne, 2001: Purification and Characterization of meta-Cresol Purple for Spectrophotometric Seawater pH Measurements, *Envir. Sci and Tech*., **45**, 4862-4868. DOI:10.1021/es2006665d

Marinenko, G., and J.K. Taylor, 1968: Electrochemical equivalents of benzoic and oxalic acid. *Anal. Chem.*, **40**, 1645-1651.

Millero F. J., Zhang, J. Z., Fiol, S., Sotolongo, S., Roy, R., Lee, K., and Mane, S., 1993a. The use of buffers to measure the pH of seawater, *Mar. Chem.,* 44, 143-152.

Millero, F.J., R.H. Byrne, R. Wanninkhof, R. Feely, T. Clayton, P. Murphy, and M.F. Lamb, 1993a: The internal consistency of CO_2 measurements in the equatorial Pacific. *Mar. Chem.*, **44**, 269-280.

Millero, F.J., J.-Z. Zhang, K, Lee, and D.M. Campbell, 1993b: Titration alkalinity of seawater. *Mar. Chem.*, **44**, 153-165.

Millero, F.J.. T. Graham, F. Huang, H. Bustos, and D. Pierrot, 2006, Dissociation constants for carbonic acid in seawater as a function of temperature and salinity, Mar. Chem., **100,** 80-94.

Pierrot, D., E. Lewis, D.W.R. Wallace, 2006. MS Excel Program Developed for CO2 System Calculations. ORNL/CDIAC-105a Carbon Dioxide Information Analysis Center, Oak Ridge National Laboratory, U.S. Department of Energy, Oak Ridge, Tennessee. http://dx.doi.org/10.3334/CDIAC/otg.CO2SYS_XLS_CDIAC105a.

Ramette, R. W., C. H. Culberson, and R. G. Bates 1977. Acid base properties of tris (hydroxymethyl) aminomethane (tris) buffers in seawater from 5 to 40^{o}C. *Analytical Chemistry*, 49, 867-870.

Schlitzer, R., Ocean Data View 4, http://odv.awi.de, 2012.

Taylor, J.K., and S.W. Smith, 1959: Precise coulometric titration of acids and bases. *J. Res. Natl. Bur. Stds.*, **63**, 153-159.

Appendices

A. Waypoint coordinates and bottom depth of the A16 2013/14 cruise.

A16 North

Station	Date	Latitude	Longitude	Depth
1	8/3/2013	63.3011	-20.001	197
2	8/4/2013	63.2173	-20.0014	559
3	8/4/2013	63.1167	-20.0018	985
4	8/4/2013	62.7506	-19.9975	1411
5	8/4/2013	62.3319	-19.9977	1807
6	8/4/2013	61.8329	-19.9991	1711
7	8/5/2013	61.6141	-19.9961	2052
8	8/5/2013	61.3326	-19.9947	2356
9	8/5/2013	60.9981	-20.0049	2404
10	8/5/2013	60.4994	-20.0003	2534
11	8/5/2013	60.0002	-19.9985	2726
12	8/6/2013	59.4972	-19.9973	2772
13	8/6/2013	58.9993	-19.9991	2844
14	8/6/2013	58.4995	-19.9983	2572
15	8/6/2013	58.0017	-20.0016	1637
16	8/7/2013	57.5002	-19.999	1167
17	8/7/2013	57.0009	-20.0015	977
18	8/7/2013	56.4998	-19.9997	1371
19	8/7/2013	55.9999	-19.9998	1461
20	8/7/2013	55.501	-19.9996	1097
21	8/8/2013	54.9992	-19.9934	1649
22	8/8/2013	54.4991	-20.0005	1382
23	8/8/2013	53.9986	-19.9983	1419
24	8/8/2013	53.5008	-19.9968	2290
25	8/8/2013	52.9995	-20.0001	2678
26	8/9/2013	52.4999	-20.0009	2779
27	8/9/2013	51.9957	-20.0003	3758
28	8/9/2013	51.5016	-19.9998	3638
29	8/10/2013	50.9996	-20.0009	3670
30	8/10/2013	50.4980	-19.9919	3937
31	8/10/2013	49.9994	-19.9997	4408
32	8/10/2013	49.5084	-20.0015	3919
33	8/11/2013	49.0003	-19.9906	4413
34	8/11/2013	48.4993	-19.9996	4046
35	8/11/2013	47.9997	-20.0008	4367
36	8/12/2013	47.4787	-19.9970	4565

Appendix A Cont.

Station	Date	Latitude	Longitude	Depth
37	8/12/2013	46.9985	-19.9929	4544
38	8/12/2013	46.4994	-20.0001	4878
39	8/12/2013	46.0023	-20.0005	4851
40	8/13/2013	45.4982	-19.9999	4559
41	8/13/2013	44.9997	-20.0005	4319
42	8/13/2013	44.4983	-19.9967	-999
43	8/14/2013	43.9989	-20.0013	4016
44	8/14/2013	43.5003	-20.0032	4009
45	8/14/2013	42.9989	-19.9991	5168
46	8/14/2013	42.5032	-19.9975	4197
47	8/15/2013	41.9999	-19.9997	2379
48	8/15/2013	41.4988	-19.9938	2737
49	8/15/2013	40.9993	-19.9999	4716
50	8/15/2013	40.5002	-20.0015	4929
51	8/16/2013	40.0000	-19.9997	4774
52	8/16/2013	39.4990	-19.9996	4680
53	8/16/2013	38.9992	-19.9991	4762
54	8/17/2013	38.4999	-19.9994	4244
55	8/17/2013	38.0029	-20.0056	5125
56	8/17/2013	37.5040	-20.0012	4842
57	8/18/2013	36.9993	-19.9996	3828
58	8/18/2013	36.5005	-20.0026	5176
59	8/18/2013	35.9998	-19.9994	5370
60	8/18/2013	35.4993	-20.2844	5286
61	8/19/2013	35.0007	-20.5664	5129
62	8/19/2013	34.5008	-20.8503	5183
63	8/19/2013	34.0018	-21.1303	5250
64	8/20/2013	33.4995	-21.3998	5349
65	8/20/2013	32.9994	-21.6835	5271
66	8/20/2013	32.5018	-21.9664	5220
67	8/21/2013	32.0001	-22.2501	5184
68	8/21/2013	31.5001	-22.5339	5238
69	8/21/2013	31.0003	-22.8182	5254
70	8/22/2013	30.5005	-23.0993	5296
71	9/3/2013	30.4997	-23.1016	5294
72	9/3/2013	30.0008	-23.3668	5260
73	9/4/2013	29.5025	-23.6518	5247
74	9/4/2013	28.9998	-23.9350	5208

Appendix A Cont.

Station	Date	Latitude	Longitude	Depth
75	9/4/2013	28.4996	-24.2167	-999
76	9/5/2013	28.0022	-24.5034	5239
77	9/5/2013	27.4998	-24.7842	5212
78	9/5/2013	27.0007	-25.0661	5256
79	9/5/2013	26.5015	-25.3517	5268
80	9/6/2013	25.9986	-25.6324	4496
81	9/6/2013	25.4994	-25.9012	5372
82	9/6/2013	25.0004	-26.1834	5414
83	9/7/2013	24.5683	-26.4323	5434
84	9/7/2013	23.9997	-26.7504	5475
85	9/7/2013	23.5024	-27.0345	5523
86	9/8/2013	23.0006	-27.3157	5542
87	9/8/2013	22.4997	-27.5992	5505
88	9/9/2013	22.0024	-27.8872	5469
89	9/9/2013	21.4998	-28.1503	5364
90	9/9/2013	20.9997	-28.4331	5089
91	9/9/2013	20.5043	-28.7185	5165
92	9/12/2013	17.4916	-29.0004	4677
93	9/13/2013	18.2499	-29.0021	4661
94	9/13/2013	18.9999	-29.0001	4586
95	9/14/2013	19.7514	-28.9983	4764
96	9/15/2013	17.0074	-28.9996	4879
97	9/15/2013	16.3325	-28.9988	5132
98	9/16/2013	15.6684	-28.9944	5181
99	9/18/2013	14.9999	-29.0000	5319
100	9/19/2013	14.3324	-28.9999	5419
101	9/19/2013	13.6658	-29.0007	5545
102	9/19/2013	13.0023	-29.0002	5720
103	9/20/2013	12.3341	-29.0004	5677
104	9/20/2013	11.6661	-29.0014	5606
105	9/20/2013	11.0103	-28.9923	5993
106	9/21/2013	10.5009	-28.7487	5392
107	9/21/2013	10.0004	-28.5005	5373
108	9/21/2013	9.5009	-28.2506	5424
109	9/22/2013	8.9996	-27.9983	5224
110	9/22/2013	8.5007	-27.7505	4955
111	9/22/2013	8.0000	-27.4999	5102
112	9/22/2013	7.5015	-27.2498	4640

Appendix A cont.

Station	Date	Latitude	Longitude	Depth
113	9/23/2013	7.0003	-26.9987	4380
114	9/23/2013	6.5006	-26.7509	4663
115	9/23/2013	5.9970	-26.5050	4307
116	9/24/2013	5.5000	-26.2509	4267
117	9/24/2013	4.9988	-26.0000	4536
118	9/24/2013	4.5017	-25.7479	4096
119	9/25/2013	4.0027	-25.5025	4043
120	9/25/2013	3.5002	-25.2505	4139
121	9/25/2013	3.0000	-25.0000	4426
122	9/25/2013	2.6675	-25.0000	4103
123	9/26/2013	2.3334	-25.0010	3774
124	9/26/2013	1.9997	-25.0004	3890
125	9/26/2013	1.6652	-25.0006	3829
126	9/26/2013	1.3336	-25.0003	3641
127	9/27/2013	1.0159	-25.0002	3144
128	9/27/2013	0.6666	-25.0002	4445
129	9/27/2013	0.3348	-24.9989	3597
130	9/27/2013	-0.0008	-24.9899	3100
131	9/27/2013	-0.3323	-25.0022	3055
132	9/28/2013	-0.6661	-25.0006	3219
133	9/28/2013	-0.9959	-24.9977	3063
134	9/28/2013	-1.3326	-25.0002	4735
135	9/28/2013	-1.6654	-24.9996	4951
136	9/29/2013	-1.9992	-24.9992	4967
137	9/29/2013	-2.3332	-24.9995	5048
138	9/29/2013	-2.6669	-25.0002	5378
139	9/29/2013	-2.9998	-24.9996	5373
140	9/30/2013	-3.4996	-24.9994	5576
141	9/30/2013	-3.9999	-24.9982	5352
142	9/30/2013	-4.4989	-25.0000	5558
143	10/1/2013	-4.9995	-25.0005	5698
144	10/1/2013	-5.4995	-24.9998	5687
145	10/1/2013	-5.9982	-25.0001	5814

Appendix A cont.

A16 South

Station	Date	Latitude	Longitude	Depth
1	12/26/2013	-6.0016	-24.9998	5809
2	12/26/2013	-6.4977	-24.9999	5628
3	12/26/2013	-6.9988	-25.0043	5578
4	12/27/2013	-7.4997	-25.0000	5795
5	12/27/2013	-7.9989	-24.9992	5709
6	12/27/2013	-8.4998	-24.9999	5739
7	12/28/2013	-8.9992	-25.0001	5691
8	12/28/2013	-9.5006	-24.9968	5783
9	12/28/2013	-10.0004	-25.0001	5406
10	12/29/2013	-10.4998	-24.9998	5427
11	12/29/2013	-10.9990	-24.9999	5417
12	12/29/2013	-11.4998	-24.9998	4331
13	12/30/2013	-11.9984	-24.9999	5808
14	12/30/2013	-12.5005	-25.0001	5587
15	12/30/2013	-12.9992	-24.9997	5778
16	12/30/2013	-13.5000	-25.0003	5158
17	12/31/2013	-14.0001	-25.0002	5922
18	12/31/2013	-14.5005	-25.0008	5405
19	12/31/2013	-15.0000	-25.0001	5247
20	1/1/2014	-15.4994	-24.9999	4995
21	1/1/2014	-16.0005	-25.0015	5657
22	1/1/2014	-16.5003	-25.0001	5118
23	1/2/2014	-17.0000	-25.0000	5279
24	1/2/2014	-17.5023	-25.0000	5172
25	1/2/2014	-18.0003	-25.0001	5564
26	1/3/2014	-18.5002	-25.0001	5471
27	1/3/2014	-18.9973	-25.0017	5816
28	1/3/2014	-19.5005	-25.0001	5460
29	1/4/2014	-19.9995	-24.9979	6028
30	1/4/2014	-20.5001	-25.0001	5433
31	1/4/2014	-21.0019	-25.0041	5231
32	1/4/2014	-21.5005	-25.0001	5330
33	1/5/2014	-21.9998	-25.0001	5133
34	1/5/2014	-22.4999	-24.9999	5533
35	1/5/2014	-22.9993	-24.9997	5114
36	1/6/2014	-23.5002	-25.0002	5435
37	1/6/2014	-23.9999	-25.0002	5619

Appendix A Cont.

Station	Date	Latitude	Longitude	Depth
38	1/6/2014	-24.5000	-25.0000	5217
39	1/7/2014	-25.0005	-25.0004	5430
40	1/7/2014	-25.4961	-25.0047	4981
41	1/7/2014	-26.0001	-25.0001	4897
42	1/8/2014	-26.5011	-25.0014	4765
43	1/8/2014	-26.9998	-25.0002	4721
44	1/8/2014	-27.5007	-25.0049	4848
45	1/8/2014	-28.0001	-25.0002	5323
46	1/9/2014	-28.5005	-25.0021	5307
47	1/9/2014	-28.9993	-25.0018	5031
48	1/9/2014	-29.5003	-25.0000	5348
49	1/10/2014	-30.0002	-24.9975	5593
50	1/10/2014	-30.5004	-24.9996	4675
51	1/10/2014	-31.0033	-25.0006	4537
52	1/10/2014	-31.5004	-25.0003	4494
53	1/11/2014	-32.0005	-25.0001	4321
54	1/11/2014	-32.5003	-24.9995	4158
55	1/11/2014	-33.0001	-25.0000	4586
56	1/12/2014	-33.4968	-24.9985	4388
57	1/12/2014	-34.0002	-25.0005	4079
58	1/12/2014	-34.4997	-24.9993	3973
59	1/12/2014	-34.9977	-24.9999	4115
60	1/13/2014	-35.4999	-25.0001	4113
61	1/13/2014	-36.0000	-25.3001	4039
62	1/13/2014	-36.4999	-25.6001	4093
63	1/14/2014	-36.9994	-25.8994	4126
64	1/14/2014	-37.4994	-26.2003	4195
65	1/14/2014	-38.0000	-26.4387	4068
66	1/15/2014	-38.4986	-26.8670	4173
67	1/15/2014	-38.9946	-27.1611	4138
68	1/15/2014	-39.5001	-27.4849	4502
69	1/16/2014	-39.9986	-27.8001	4301
70	1/16/2014	-40.4996	-28.1006	4360
71	1/16/2014	-41.0119	-28.4048	4328
72	1/16/2014	-41.5003	-28.7157	4355
73	1/17/2014	-41.9999	-29.0328	4437
74	1/17/2014	-42.5005	-29.3474	4506
75	1/18/2014	-43.0043	-29.6443	4479

Appendix A Cont.

Station	Date	Latitude	Longitude	Depth
76	1/18/2014	-43.4997	-29.9633	4689
77	1/19/2014	-44.0015	-30.2636	4620
78	1/19/2014	-44.5001	-30.5832	5106
79	1/19/2014	-45.0000	-30.9042	4817
80	1/19/2014	-45.4912	-31.1853	5094
81	1/20/2014	-45.9991	-31.5130	5262
82	1/20/2014	-46.4987	-31.8079	5240
83	1/20/2014	-46.9993	-32.1241	5179
84	1/21/2014	-47.5084	-32.4574	5352
85	1/21/2014	-48.0071	-32.7767	5325
86	1/21/2014	-48.5033	-33.0671	4961
87	1/22/2014	-49.0065	-33.3690	4940
88	1/22/2014	-49.5041	-33.6723	5176
89	1/23/2014	-50.0008	-34.0001	5043
90	1/23/2014	-50.5013	-34.2981	4892
91	1/23/2014	-51.0004	-34.6145	5000
92	1/24/2014	-51.4994	-34.9314	4816
93	1/24/2014	-52.0000	-35.2330	4453
94	1/25/2014	-52.4998	-35.5500	3868
95	1/25/2014	-53.0009	-35.8472	3526
96	1/25/2014	-53.2570	-36.0277	3295
97	1/25/2014	-53.4317	-36.1152	2716
98	1/26/2014	-53.5942	-36.2107	1779
99	1/26/2014	-53.7400	-36.2431	923
100	1/26/2014	-53.8502	-36.3832	219
101	1/26/2014	-55.2302	-34.7378	177
102	1/26/2014	-55.2677	-34.6293	941
103	1/26/2014	-55.3296	-34.5295	1836
104	1/27/2014	-55.5994	-34.1827	2210
105	1/27/2014	-55.9992	-33.6328	2552
106	1/27/2014	-56.5001	-32.9482	3719
107	1/28/2014	-56.9988	-32.2876	3703
108	1/28/2014	-57.4997	-31.5992	3399
109	1/28/2014	-58.0281	-30.9118	3554
110	1/28/2014	-58.5010	-30.9296	2926
111	1/29/2014	-58.9991	-30.9237	3093
112	1/29/2014	-59.5011	-30.9186	3683
113	1/30/2014	-60.0130	-30.8953	-999

B. Scientific Personnel.

Scientific Personnel CLIVAR/Carbon A16N_2013 Leg I	
Role	**Name (affiliation)**
Chief Scientist	Molly Baringer (AOML)
Co-Chief Scientist	Denis Volkov (AOML)
Data Management	Courtney Schatzman (SIO)
CTD Processing	Kristy McTaggert (PMEL)
CTD/Salinity/LADCP/ET	Andrew Stefanick (AOML)
CTD/Salinity/LADCP	James Hooper (AOML)
CTD Watch	Christine Mann (CSU)
CTD Watch	Ashley Wheeler (CSU)
CTD Watch/14C	Brett Walker (UCI)
CTD/LADCP	Oyvind Lundesgaard (UH)
Dissolved O2	Christopher Langdon (RSMAS)
Dissolved O2	Laura Stoltenberg (RSMAS)
Nutrients	Eric Weisgarver (PMEL)
Nutrients	Charles Fischer (AOML)
Total CO2 (DIC)	Robert Castle (AOML)
Total CO2 (DIC)	Charles Featherstone (AOML)
CFCs/SF6	David Wisegarver (PMEL)
CFCs/SF6/18O	Jennifer Hertzberg (TAMU)
pCO2	Kevin Sullivan (AOML/CIMAS)
Total Alkalinity/pH	Ryan Woosley (RSMAS)
Total Alkalinity/pH	Josh Levy (RSMAS)
Total Alkalinity/pH	James Williamson (RSMAS)
Total Alkalinity/pH	Jennifer Byrne (RSMAS)
Trace Metals	Joseph Resing (UW)
Trace Metals	William Landing (FSU)
Trace Metals	Rachel Shelley (FSU)

Appendix B Cont.

Role	***Name (affiliation)***
Trace Metals	*Pam Barrett (UW)*
Helium/Tritium/18O	Anthony Dachille (LDEO)
DOC, and 14C and 13C of DIC	Monica Mejia (RSMAS)
CDOM	Erik Stassinos (UCSB)
Scientific Personnel CLIVAR/Carbon A16N_2013 Leg II	
Chief Scientist	John Bullister (PMEL)
Co-Chief Scientist	Rolf Sonnerup (UW)
Data Management	Courtney Schatzman (SIO)
CTD Processing	Kristy McTaggert (PMEL)
CTD/Salinity/LADCP/ET	Andrew Stefanick (AOML)
CTD/Salinity/LADCP	James Hooper (AOML)
CTD Watch	Katie Kirk (WHOI)
CTD Watch	Joseph Schoonover (FSU)
CTD Watch/14C	Martine Stueben (RSMAS)
CTD/LADCP	Oyvind Lundesgaard (UH)
Dissolved O2	Christopher Langdon (RSMAS)
Dissolved O2	Laura Stoltenberg (RSMAS)
Nutrients	Eric Weisgarver (PMEL)
Nutrients	Charles Fischer (AOML)
Total CO2 (DIC)	Robert Castle (AOML)
Total CO2 (DIC)	Charles Featherstone (AOML)
CFCs/SF6	David Wisegarver (PMEL)
CFCs/SF6/	Kyra Freeman (UCSD)
pCO2	Leticia Barbero (AOML/CIMAS)
Total Alkalinity/pH	Carmen Rodriguez (RSMAS)

Appendix B Cont.

Role	***Name (affiliation)***
Total Alkalinity/pH	Josh Levy (RSMAS)
Total Alkalinity/pH	James Williamson (RSMAS)
Total Alkalinity/pH	Kristen Mastropole (RSMAS)
Trace Metals	Peter Morton (FSU)
Trace Metals	Pam Barrett (UW)
Trace Metals	Nathan Buck (PMEL)
Trace Metals	Randy Morton (FSU)
Helium/Tritium/18O	Anthony Dachille (LDEO)
DOC, and 14C and 13C of DIC	Monica Mejia (RSMAS)
CDOM	Eli Aghassi (UCSB)

Scientific Personnel RB 13-07-2014 A16S Cruise

Role	**Name (affiliation)**
Chief Scientist	Rik Wanninkhof (AOML)
Co-Chief Scientist	Leticia Barbero (AOML/CIMAS)
Data Management	Alex Quintero (SIO)
CTD	Kristy McTaggert (PMEL)
CTD watch-stander	Jonathan Christophersen (FSU)
CTD watch-stander	Gabrielle Weiss (U Hawaii)
LADCP	Lora Van Uffelen (U Hawaii)
LADCP/Salinity	Jay Hooper (AOML/CIMAS)
Salinity	Ed Hunt (Contract)
O2	Laura Stoltenberg (RSMAS)
O2	Andrew Stefanick (AOML)
Nutrients	Eric Wisegarver (PMEL)
Nutrients	Charles Fischer (AOML)
DIC	Robert Castle (AOML)
DIC	Julie Arrington (PMEL)
Total Alkalinity/pH	Ryan Woosley (RSMAS)

Appendix B Cont.

Role	***Name (affiliation)***
Total Alkalinity/pH	*Carmen Rodriguez (RSMAS)*
Total Alkalinity/pH	Julie Paine (RSMAS)
Trace Metals	William Landing (FSU)
Trace Metals	Rachel Shelley (FSU)
Trace Metals	Chris Measures (U Hawaii)
Trace Metals	Mariko Hatta (U Hawaii)
CFCs/SF6	David Wisegarver (PMEL)
CFCs/SF6	Patrick Mears (U Texas)
Helium/Tritium	Anthony Dachille (LDEO)
DOM/DI14C/DOC	Valentina Caccia (WHOI)
Chipod	Byungho Lim (OSU)

C. Diagram of an automated total alkalinity system

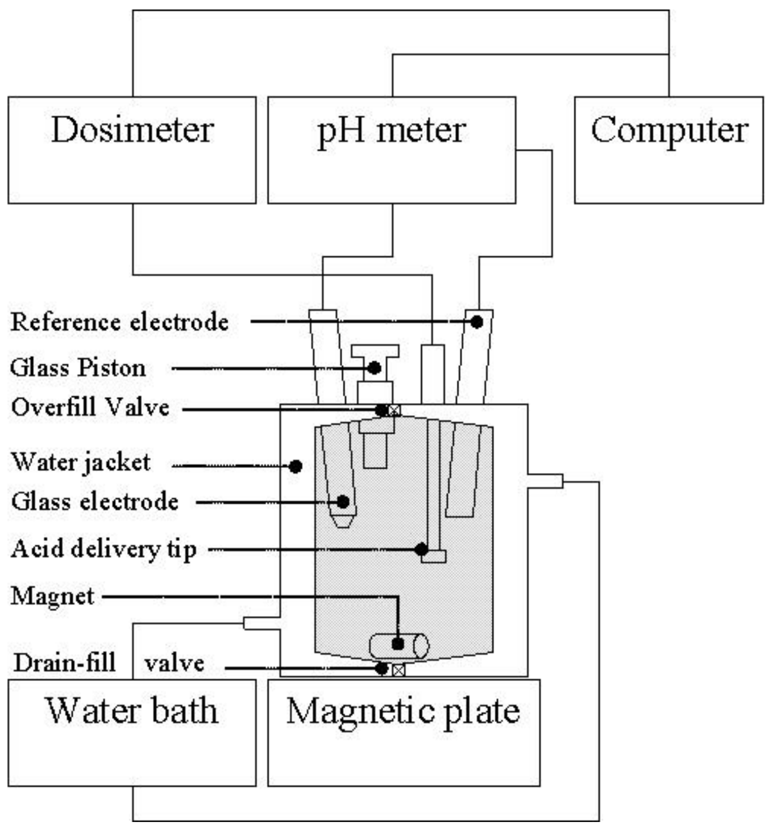

D. Diagram of a manual pH system

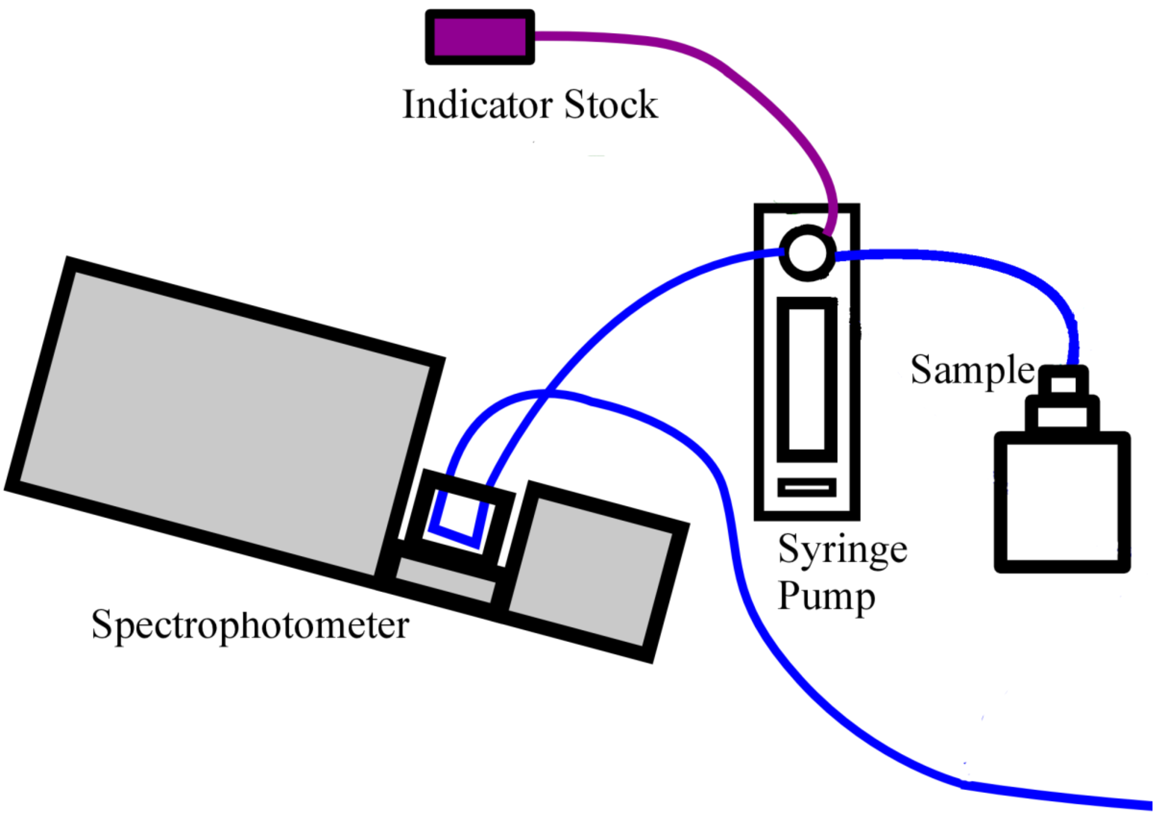

E. Data format description

FIELD NAME	DESCRIPTION	UNITS
Lat	Latitude	º N
Lon	Longitude	º E
Depth	Depth	m
P	Pressure	db
S	Salinity	S_p
T	Temperature	º C
ϑ	Potential Temperature	º C
pH_{pot}	Potentiometric pH	
pH_{spec}	Spectrophotemetric pH	
TA	Total Alkalinity	$\mu mol \cdot kg^{-1}$
TCO_2	Total Inorganic Carbon Dioxide	$\mu mol \cdot kg^{-1}$
NTA	Normalized TA to a salinity of 35	$\mu mol \cdot kg^{-1}$
$NTCO_2$	Normalized TCO_2 to a salinity of 35	$\mu mol \cdot kg^{-1}$